



**POLITECNICO DI TORINO**  
**COLLEGIO DI INGEGNERIA CIVILE**

---

*Corso di Laurea Magistrale in Ingegneria Civile*

**CONTROL CRACK WIDTH  
IN HYBRID OPTIMISED FLAT SLAB**

*Relatore*

**Prof. Pasquale Fantilli**

*Laureanda*

**Manuela Valerio**

*Co-relatori*

**Prof. Albert De la Fuente  
PhD(c) Stanislav Aidarov**

---

ANNO ACCADEMICO 2018/2019

This thesis was developed at  
Smart Engineering Bcn, Engineering company and  
Spin-off of UPC-Universitat Politècnica de Catalunya  
in collaboration with Polytechnic of Turin.  
Barcelona-Torino, October 2019





*"...per chi viaggia in direzione ostinata e contraria..."*  
Smisurata Preghiera - F. De Andrè

*Dedicato alla mia Famiglia  
e a quelle nate in questi anni,  
lontano da casa*



# Contents

<b>1</b>	<b>Introduction</b>	<b>1</b>
1.1	The durability problem . . . . .	1
1.2	Objective . . . . .	2
<b>2</b>	<b>State of art</b>	<b>3</b>
2.1	Fibre reinforced concrete . . . . .	3
2.2	Fibre types . . . . .	4
2.3	Steel fibres . . . . .	6
2.4	Constitutive laws . . . . .	7
2.4.1	Plane strain: ordinary reinforced concrete . . . . .	8
2.4.2	Plane strain: fibre reinforced concrete . . . . .	9
2.4.3	Conventional concrete . . . . .	10
2.4.4	Fibre Reinforced Concrete . . . . .	14
2.4.5	Multilinear Model for FRC . . . . .	18
2.4.6	Classification of fibres . . . . .	21
<b>3</b>	<b>Control crack</b>	<b>25</b>

3.1	Cracking model in ordinary reinforced concrete . . . . .	26
3.1.1	Cracking stages, transfer length, crack spacing . . . . .	28
3.2	Cracking in FRC . . . . .	30
3.2.1	Transfer length and crack spacing . . . . .	30
3.3	Mean steel strain . . . . .	32
3.4	Estimation of crack width for FRC . . . . .	33
<b>4</b>	<b>Definition of M-N envelopes</b>	<b>35</b>
4.1	M-N envelopes at ULS for FRC . . . . .	36
4.2	M-N envelopes at SLS for FRC . . . . .	37
4.3	Comparison of the results at ULS and SLS . . . . .	39
4.4	Effect of fibres on behaviour of the material (M-N envelope) .	40
<b>5</b>	<b>Case study</b>	<b>43</b>
5.1	Model definition: flat slab . . . . .	43
5.2	Hybrid Solution for flat slabs at ULS . . . . .	45
5.2.1	Plastic analysis and Yield-Line Theory . . . . .	45
5.2.2	Optimization of hybrid reinforcement for flat slabs . . .	48
5.3	Hybrid Solution for flat slabs at SLS . . . . .	50
5.3.1	Calculation plane deformation and crack width . . . . .	52
5.4	Results . . . . .	52
5.5	Crack Width Limits at SLS . . . . .	59
5.6	Comparison of achieved results with permitted crack widths .	60
5.7	Design of additional steel reinforcement at SLS . . . . .	63

<i>CONTENTS</i>	ix
5.8 Total steel content at SLS . . . . .	67
5.9 Stress limitations . . . . .	72
5.10 Economic aspect . . . . .	74
<b>6 Conclusion and future studies</b>	<b>77</b>
6.1 Conclusions about use of fibre . . . . .	77
6.2 Future studies . . . . .	78
<b>Annexes</b>	<b>78</b>
Annex A: Newton Raphson algorithm . . . . .	78
<b>Acronyms</b>	<b>85</b>
<b>List of figures</b>	<b>90</b>
<b>List of tables</b>	<b>92</b>
<b>Bibliography</b>	<b>94</b>
<b>Acknowledgements</b>	<b>95</b>



## Abstract

The development of relevant standards and guidelines have boosted the implementation of steel fibre reinforced concrete in elements with high structural responsibility. Nowadays, this technological material is already considered as an alternative solution for certain structural elements and elevated slabs are among those. The total substitution of conventional reinforcement was achieved in several cases throughout the world demonstrating clear advantages of this approach, such as reduction of execution time, optimisation of resources, reduction of negative environmental and other social impacts.

Despite the proven benefits of Steel Fibre Reinforced Concrete (SFRC) application for elevated slabs, the hybrid solutions (rebars + FRC) were also studied due to possibility of decreasing the fibre content in concrete mix providing the traditional reinforcement in the zones with particularly high stresses. Therefore, the potential implementation of Hybrid Reinforced Concrete (HRC) could be even more attractive from the technical point of view (reduction of total amount of steel and providing the better crack width control).

Nowadays, several studies have been carried out in order to evaluate the structural capacity of HRC elevated slabs. However, most of them were focused on the behaviour the abovementioned plane elements at Ultimate Limit States (SLS), neglecting the study of the structural requirements at Serviceability Limit States. Taking this into account, the design approach for crack width estimation has been developed for HRC solutions which, in turn, will provide the additional factor during the assessment of best traditional reinforcement / steel fibre content ratio for this type of structures.



## Abstract

L'elaborazione di norme tecniche e linee guida riguardanti i calcestruzzi fibrorinforzati ha stimolato l'utilizzo di questi ultimi in elementi ad alta responsabilità strutturale. Questo materiale innovativo è già oggi considerato una soluzione alternativa per alcuni elementi strutturali, come le piastre. La sostituzione totale del rinforzo convenzionale è stata raggiunta, in diversi casi e in tutto il mondo, dimostrando evidenti vantaggi di questo approccio, come: la riduzione dei tempi di esecuzione, l'ottimizzazione delle risorse, la riduzione degli impatti ambientali e sociali negativi.

Nonostante i comprovati benefici dell'applicazione del calcestruzzo fibrirrinforzato per gli elementi piastra, sono state studiate anche le soluzioni ibride (barre + fibrorinforzo) grazie alla possibilità di diminuire il contenuto di fibre nel conglomerato cementizio e aggiungere il tradizionale rinforzo, nelle zone con sollecitazioni particolarmente elevate. Pertanto, la potenziale implementazione di soluzioni ibride potrebbe essere ancora più interessante dal punto di vista tecnico e in particolare nella riduzione del contenuto totale di acciaio e nel controllo dell'apertura delle fessure.

Attualmente sono stati condotti diversi studi per valutare la capacità strutturale delle solette ibride. Tuttavia, la maggior parte di essi si sono concentrati sul comportamento dell'elemento allo Stato Limite Ultimo, trascurando la possibile risposta strutturale allo Stato Limite di Esercizio. Tenendo conto di ciò, è stata sviluppata una procedura di progettazione per la valutazione della larghezza delle fessure al fine di valutare più in dettaglio le soluzioni ibride per le solette sopraelevate che, a loro volta, consentiranno di trovare il miglior rapporto tra rinforzo tradizionale e contenuto di fibre per questo tipo di strutture.



# Chapter 1

## Introduction

In recent decades, the construction sector has focused its development on discovery and new technological materials, in order to improve some important characteristics of concrete. In this regard, thanks to the development of guidelines and standards, the use of Fibre Reinforced Concrete (FRC) is becoming more widespread. The presence of fibres plays an important role in improving and controlling certain fundamental parameters such as durability, crack resistance, thermal characteristics, residual tensile strength, fire resistance and workability. Integrating traditional and fibre reinforcement serves to better modulate these parameters and can be advantageous from an environmental, economic and construction time point of view. These important points have allowed the use of the hybrid solution in flat slabs. However, by focusing more on the problem of the durability of a structure and, in particular, the requirements to which it must respond at Serviceability Limit State (SLS), it is necessary to know how the integration of the fiber gives higher performance to the control of the crack opening, compared to traditional concrete and if it is possible to eliminate the traditional reinforcement.

### 1.1 The durability problem

The theme of the durability of reinforced concrete works is now of great relevance and sensitivity, in the light of the latest disastrous episodes that have involved, even Italy, in the collapse of important structures. The high cost of maintaining and repairing existing structures has become a problem not only for the economy and society, but also for the environmental sustainability of

the entire construction sector. Structural durability is improved by preventing aggressive substances from entering the concrete matrix. This is possible by acting on two fronts: the first is represented by the internal porosity of the concrete, which can be reduced by lowering the water/cement ratio; the second is represented by the cracks, which represent a preferential way to reach the innermost parts of the structure. One possible solution could be to invest in the use of new materials designed specifically to improve the durability of the structural elements and give greater prospects of useful life, especially for those works exposed to particularly aggressive environments. In this context, the use of FRC can be very useful. In fact, the addition of fibres to the concrete mix makes it possible to improve its toughness characteristics: the fibres, acting as "crack arrests", limit the width of the cracks, the preferential entry of aggressive agents that cause corrosion of the reinforcements.

The current standards codes provide for a limitation of the width of the cracks which, especially for severe environmental exposure classes, force the designer to vary parameters such as the percentage of reinforcement and the size of the sections, in order to meet the requirements imposed. The use of fibres would allow a reduction in the width of the cracks without changing significant design parameters, which would lead to an increase in construction costs and greater architectural conditioning.

Different types of fibres are available on the market today: by varying materials and dimensions, it is possible to have a cracking control at different levels.

## 1.2 Objective

Taking into account the studies already carried out on the optimisation of steel quantities in hybrid solutions, the aim of this work was to focus attention on performance at SLS. First of all, it has been studied the structural response, in terms of crack opening, and then, referring to restrictive regulations in this regard, its behaviour was improved. The work carried out continues to follow the objective of finding a point of optimization between the quantities of steel used for the fiber and the bars, but at the same time seeks to integrate the fulfillment of Ultimate Limit State (ULS) and SLS criteria.

## Chapter 2

# State of art

The presence of fibres in concrete composition increases the ductility of the material providing the capacity of bearing the post-cracking tensile stresses. In fact, the incorporation of fibrous elements to enhance the properties of the brittle materials is not a novel idea – the ancient Egyptians already used straws and horsehair to reinforce mud bricks. However, the study of application of FRC for structural and non-structural purposes in its current state was started only in the early 1960's following the research work of J.P. Romualdi, J.A. Mandel and G.P. Batson in the USA [1] [2] and H. Krenchel in Denmark [3].

The cases of implementation of FRC in Europe was found in 1970's; in particular, the precast FRC pipes were executed during this period in Italy. Despite the noticeable advantages of this technological material, its spread was limited (especially in structural purposes) due to the lack of relevant standards. However, within last decades several national codes and guidelines were published which comprise the information for FRC application in the construction industry, such as DBV [4], RILEM TC 162-TDF [5], CNR-DT 204/2006 [6], EHE-08 and the Model Code 2010 [7].

### 2.1 Fibre reinforced concrete

According to definition given by American Concrete Institute (ACI) the FRC is:

*"... a concrete made primarily of hydraulic cements, aggregates, and discrete reinforcing fibres. Fibres suitable for reinforcing concrete have been produced from steel, glass, and organic polymers (synthetic fibres). Naturally occurring asbestos fibres and vegetable fibres, such as sisal and jute, are also used for reinforcement. The concrete bases may be mortars, normally proportioned mixtures, or mixtures specifically formulated for a particular application. If properly engineered, one of the greatest benefits-be gained by using fiber reinforcement is improved long-term serviceability of the structure or product."* [8]

The incorporation of fibres into cementitious matrix effects on various properties of concrete. The degree of influence depends on the physical and mechanical properties of fibres such as geometry, density and tensile strength. Also, the distribution and orientation of fibres in the concrete mix is of paramount importance in terms of the capacity of material.

Originally, the use of fibres was mainly aimed to enhance the non-structural properties of the material; cracking control, fire resistance, toughness, resistance to fatigue and impact could be improved by the presence of fibres in the material which permits to carry certain amount of tensile stresses after the cracking due to so called "bridge effect" (Figure 2.1). Nevertheless, the acceptance of this relatively new material for structural purposes within the relevant design codes and guidelines permitted to expand the field of SFRC application [9]. It is worth noting that that fibres are considered structural when they increase the value of fracture energy of matrix and their effect have to be taken in account during the strength section calculation [12]

## 2.2 Fibre types

Nowadays, certain elements with high structural responsibility were executed with partial (or even total) substitution of the traditional reinforcement which provided numerous advantages such as optimisation of the resources, reduction of execution time, reduction of environmental impacts and other social aspects. The construction of FRC elevated slabs in Spain, Estonia and Lithuania could be an illustrative example of the implementation of this technological solution [10] [11] [12].

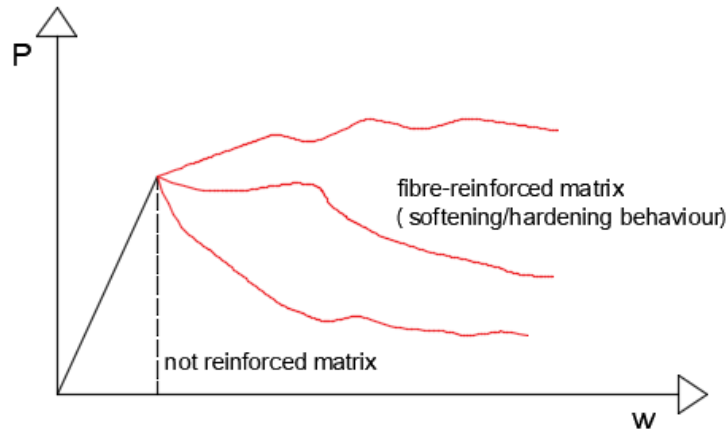


**Figure 2.1:** General diagram load/crack width for fibre-reinforced and no reinforced matrix

There are several fibre types on the market intended to meet certain design requirements which could be divided into three sub-classes, according the Table 2.1.

	Steel
Type of material	Polymeric Inorganic
Objective	Structural No structural
Dimension	Micro-fibres ( $\phi_f < 30\text{mm}$ ) Macro-fibres ( $\phi_f > 30\text{mm}$ )

**Table 2.1:** Fibre sub-classes

For the purposes of the study in question, it is important to highlight that the fibres are considered structural when they increase the value of fracture energy of matrix and their effect have to be taken in account during the strength section calculation; no structural fibres works on control width crack, fire resistance, abrasion or impact [9]. The nature and the type of fibres determine the post-cracking behaviour of the material, therefore the selection of fibre for particular purpose turns to be an essential factor for an

engineer. Nowadays, the market provides the plenty of options, varying the material, geometry and mechanical properties of fibres (Table 2.2):

Type of fiber	Equivalent diameter [mm]	Specific gravity [kg/m <sup>3</sup> ]	Tensile strength [Gpa]	Young's modulus [GPa]	Ultimate elongation %
Acrylic	0.02-0.35	1100	0.2-0.4	2	1.1
Asbestos	0.0015-0.02	3200	0.6-1	83-138	1.0-2.0
Glass	0.005-0.15	2500	1-2.6	70-80	1.5-3.5
Graphite	0.008-0.009	1900	1.26	230-415	0.5-1.0
Nylon	0.02-0.40	1100	0.76-0.82	4.1	16-20
Polyester	0.02-0.40	1400	0.72-0.86	8.3	11-13
PP	0.02-1.00	900-950	0.2-0.76	3.5-15	5.0-25.0
PVA	0.027-0.66	1300	0.9-1.6	23-40	7-8
Carbon	1400	4000	0.23-0.24	1.4	1.8
Rayon	0.02-0.38	1500	0.4-0.6	6.9	10-25
Polyethylene	0.025-1.0	960	0.2-0.3	5.0	3.0
Steel	0.15-1.00	7840	0.35-3	200	4-10

**Table 2.2:** A compilation of mechanical properties of commonly used fibres in concrete materials[8]

This variety of such essential properties as tensile strength, Young modulus and geometry of fibres provides the opportunity to pick the specific fibre type on the basis of project requirements.

## 2.3 Steel fibres

Steel fibres are generally made of carbon steel or stainless steel, where the latter is used in elements with highly demanded corrosion resistance. Tensile strength may be in the range of 345-3000 MPa, while the ultimate elongation could be up to 10% (Table 2.2). Also, the geometry of steel fibres has a considerable effect on the post-cracking behaviour. The originally used straight, smooth steel fibre is rarely seen nowadays in normal-strength concrete due to its insufficient bond with matrix [13]. Recently, fibres with end-hooks have been studied in detail due to enhanced anchorage in concrete matrix in comparison with the twisted fibres or the one with the paddles. Summarizing, the main parameters to be considered of the steel fibres are:

1. Aspect ratio: the relationship between the fibre length ( $l_f$ ) and fibre

diameter ( $\phi_f$ ). The higher the slenderness, the lower the dosage of fibres to be used;

2. Tensile strength: depends on the quality of steel and carbon content;
3. Geometry and shape: important for the adherence and anchorage (Figure 2.2).

The  $l_f$  of steel fibre is usually 2-4 times of the maximum aggregate size. The relationship between the maximum size of the coarse aggregate and  $l_f$  has more influence on flexural resistance, the workability, concrete rather its toughness influences the and toughness.

In addition, it could be highlighted that for the appropriate pouring of SFRC the length of fibre should be less than  $2/3$  of the pipe diameter. However, the length of the fibre must be sufficient to provide the appropriate adhesion with the concrete matrix in order to avoid the occurrence of the premature pull-out.

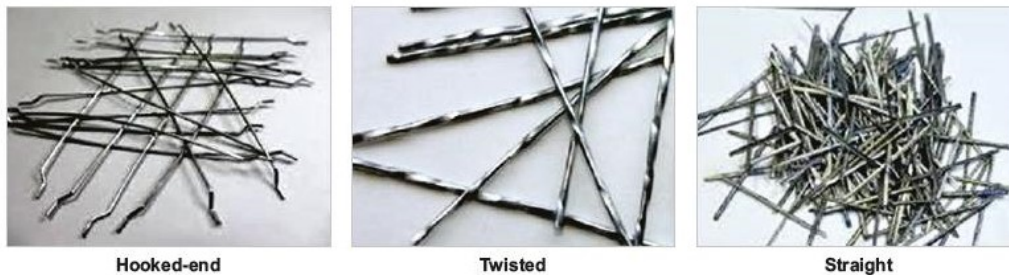


**Figure 2.2:** Types fibres steel

## 2.4 Constitutive laws

The general idea underlying the proposed models is that the contributions of steel and concrete to sectional stiffness can be separated into two constitutive laws. The moment/curvature law for each section will be obtained by non-linear sectional analysis. When defining the constitutive laws, there are values that are related to the materials, while there are others that are intrinsically related to the geometry of the section: these are, for instance, the values related to tension stiffening for steel rebars or fibre characteristic

length ( $l_{cs}$ ), for tensional behaviour of FRC. The assumptions that will be made for the constitutive models are:

1. Sections perpendicular to the axis of bending, that are plane before bending, remain plane after bending, according to Bernoulli's hypothesis;
2. There is a perfect bond between steel and concrete and the bond remains once the fibres are added to the concrete mix;
3. Tension stiffening is constant, not deteriorating with increasing load, and expressed as a fraction of the tensile stress at cracking of the effective tensile tie;
4. Bridging action of fibres in the crack is taken into account with a *classical smeared approach*; the stress ( $\sigma$ )-strain ( $\varepsilon$ ); law[14] is derived from the 3-point bending test and spread along the characteristic structural length  $l_{cs}$ ;
5. When cracking occurs, the stress of steel goes up to the maximum steel stress in a crack formation stage ( $\sigma_{sr}$ );

### 2.4.1 Plane strain: ordinary reinforced concrete

The plane strain is calculated in a range that has as maximum values ones for ULS section, in other words for the compression  $\varepsilon$  =ultimate strain concrete ( $\varepsilon_{cu}$ ), and for the tension  $\varepsilon$  =ultimate strain steel ( $\varepsilon_{su}$ ). However, at ULS the tensile strength of concrete is considered equal to 0 (see Figure ??). For sections without OR at ULS the relationship between  $\sigma$  and  $\varepsilon$  will be like in the Figure 2.3. At SLS will be take in account a small elastic contribution of tensile strength concrete until  $f_{ctm}$  (see Figure ??), in case of unreinforced section, values of tension bigger than  $f_{ctm}$  provides an immediate formation of cracks.

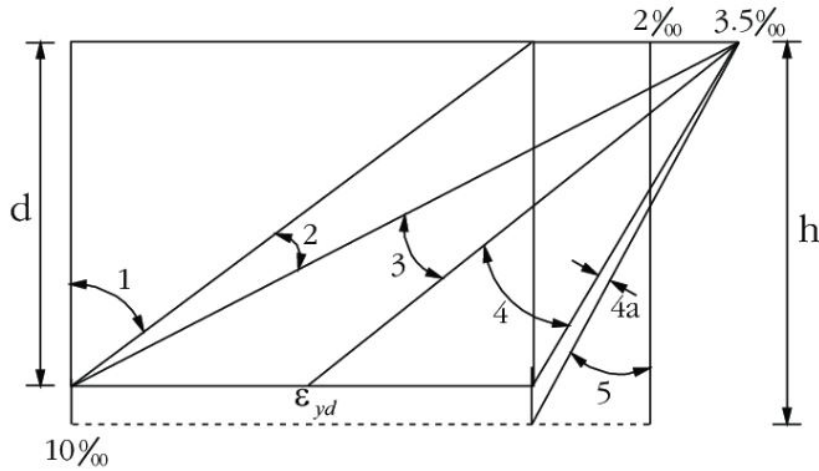


**Figure 2.3:** Plane strain for ORC

### 2.4.2 Plane strain: fibre reinforced concrete

The plain strain calculated in SFRC presents some differences in SLS and ULS case and if the reinforcement of the element is a mixed solution or not. At ULS, in presence of ordinary steel reinforcement (OR) the ultimate tensile strain is  $\varepsilon_{su}$ , but with only fibres is equal to  $\varepsilon_{ULS}$  of fibres, the strain corresponding to ultimate flexural residual strength ( $f_{Ftu}$ ). At SLS, according to fib MC10 bulletin 83 the plain strain is reduced in two limits:

1. for the compression :  $\varepsilon_{c,max}$  obtained by a reduction of compressive stress  $0.6 \cdot f_{ck}/E_c$ ;
2. for the tension:  $\varepsilon_{max}$  depends by width crack opening design ( $w_d$ ) according the following formulation:  $w_d/h$ .

Another substantial difference is in the fact that the division between the five domains of ORC is eliminated and the plan strain can be traced back to only two domains, considering : one that includes the domain 1 and 2, the other from 3 to 5.

### 2.4.3 Conventional concrete

#### Behaviour in compression

The concrete behaviour in compression is represented by specific model, based on certain properties of the material, such as  $f_{cm}$  and Young modulus. They are defined on the design compressive strength concrete ( $f_{cd}$ ) and ultimate deformation  $\varepsilon_{cu}$ . It can be chosen several constitutive diagram, according to fib Model Code 2010 (fib MC10) [14]. Within the study in question, two constitutive models have been adopted:

1. Sargin's parabolic model [7];
2. Parabola rectangle.

Sargin's parabolic model is used for both ULS and SLS, provided that equilibrium and compatibility are satisfied and adequate non-linear behaviour for materials is assumed. The analysis may be first or second order. The stress-strain relation is shown in Figure 2.4, (compressive stress and shortening strain shown as absolute values) for short term uniaxial loading is described by the Equation 2.1:

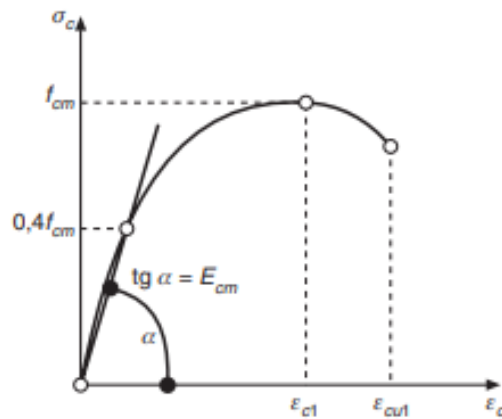


**Figure 2.4:** Schematic representation of the stress–strain relation for structural concrete [7]

$$\frac{\sigma_c}{f_{cm}} = \frac{k\eta - \eta^2}{1 + (k - 2)\eta} \quad (2.1)$$

where:

$$\eta = \frac{\varepsilon_c}{\varepsilon_{c1}} \quad (2.2)$$

$$k = \frac{1.05 \cdot E_{cm} \cdot |\varepsilon_{c1}|}{f_{cm}} \quad (2.3)$$

Other idealised stress–strain relations may be applied, if they adequately represent the behaviour of the concrete considered. The model is not linear, there is a parabolic part in it and could be appreciated in Figure 2.5.

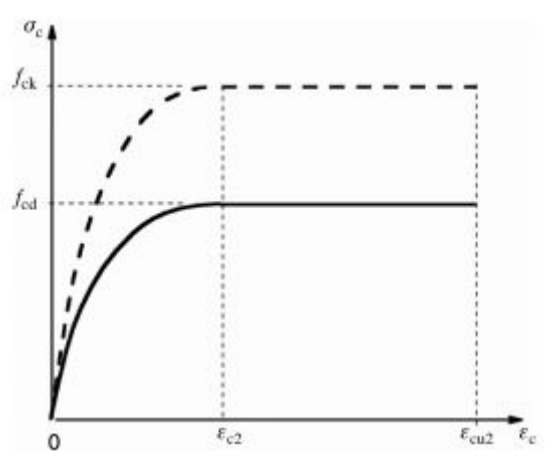


**Figure 2.5:** Parabola–rectangle diagram for concrete in compression

In fact, parabola–rectangle relation is defined according to:

$$\sigma_c = f_{cd} \cdot \left[ 1 - \left( 1 - \frac{\varepsilon_c}{\varepsilon_{c2}} \right)^n \right] \quad (2.4)$$

for  $0 \leq \varepsilon_c \leq \varepsilon_{c2}$

$$\sigma_c = f_{cd} \quad (2.5)$$

for  $\varepsilon_{c2} \leq \varepsilon_c \leq \varepsilon_{cu2}$  [14]

where:

- $n$  is the exponent;
- $\varepsilon_{c2}$  is the strain at reaching the maximum strength according;
- $\varepsilon_{cu2}$  is the the ultimate strain.

For concrete strength classes  $> C50$  the stress–strain relation is characterised by a reduced length of the horizontal plateau (Figure 2.6). For the purposes of this work, the behaviour of confined concrete was neglected, these formulas are cited in fib MC10.

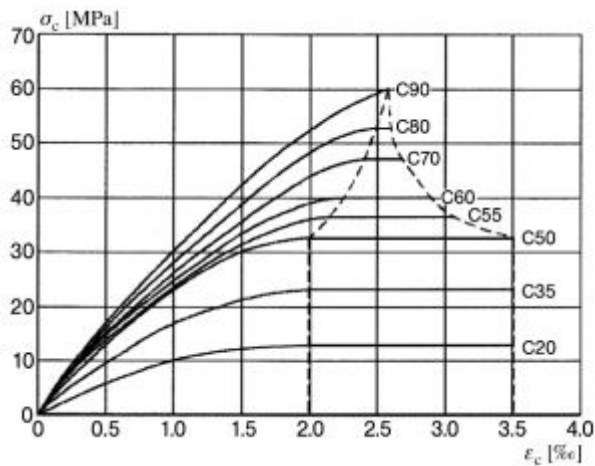


**Figure 2.6:** Design stress strain relations for various concrete strength classes

### Tensile behaviour

The concrete behaviour in tension is considered linear-elastic up to the value of mean tensile strength of concrete ( $f_{ctm}$ ). The ultimate tensile strain which corresponds to  $f_{ctm}$  could be found by means of the Young modulus of the material. In the absence of experimental data, the mean value of tensile strength  $f_{ctm}$  [Mpa] may be estimated for normal weight concrete from the  $f_{ck}$  [14]. The value of tensile strength is about 10 times less than compressive.

$$f_{ct} = 0.3 f_{ck}^{2/3} \quad (2.6)$$

## Reinforcing steel

The concrete section behaviour at tension is completely entrusted to steel reinforcement, which constitutive law represented in the Figure 2.7. In particular, it expects an elastic linear behaviour, according to Hooke, until the characteristic yield strain steel ( $\varepsilon_{yk}$ ) and a constant stress value until the ultimate characteristic strain ( $\varepsilon_{uk}$ ), depending by type of steel (see Equation 2.7 and 2.8) [14]. The equations which provides the above described law could be found below:

$$\sigma_s = E_s \cdot \varepsilon \quad (2.7)$$

for  $\varepsilon \leq \varepsilon_{yk}$

$$\sigma_s = f_{yk} \quad (2.8)$$

for  $\varepsilon > \varepsilon_{yk}$

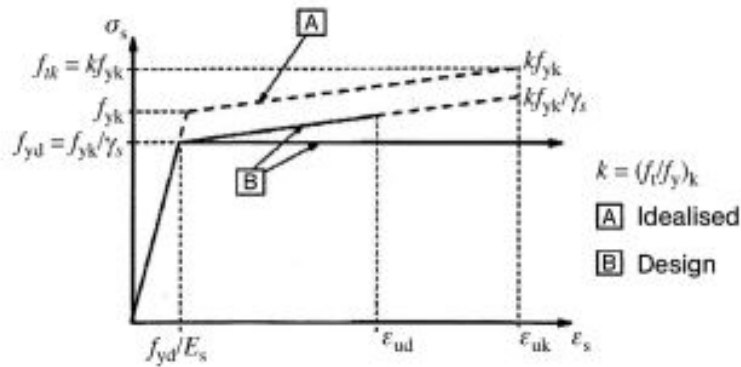
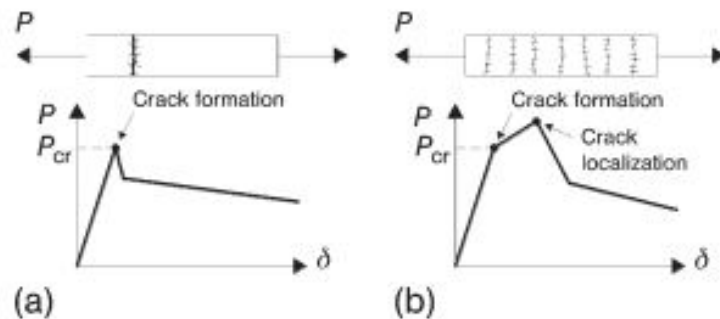


Figure 2.7: Steel behaviour

It is noteworthy to mention that each characteristic value mentioned must be appropriately reduced with a safety factor  $\gamma$  to obtain the design value. The factor  $\gamma$  has several values depending on the limit state (e.g. ULS, SLS) and the material (see Table 2.5).

### 2.4.4 Fibre Reinforced Concrete

The incorporation of fibres into the concrete mix considerably modifies the post-cracking response of the material;. Depending on fibre content, FRC can show hardening or softening behaviour under uniaxial tension. In the case of softening behaviour (Figure 2.8a) the deformations localize in one crack, while the hardening behaviour is typically characterized by the multiple cracking occurrence before reaching the peak value due to higher values of residual tensile strength in in comparison with tensile strength of concrete ( $f_{ct}$ ).



**Figure 2.8:** Softening (a) and Hardening (b) behaviour [7]

Besides the improvement of post-cracking behaviour of concrete, the presence of fibres reduces the brittleness of concrete in compression, especially in high or ultra high strength concrete. Nevertheless, in practice, the behaviour in compression is considered the same one of unreinforced material, therefore, for design purposes the above mentioned behaviour is to be taken in accordance with Chapter 2.4.1.

#### Tensile behaviour

The tension behaviour of a SFRC is the most important aspect. There are several tests to estimate the pre- and post cracking tensile strength of the material, otherwise the most utilised are bending tests. Uniaxial tensile stress, unlike compression, is not advised for standard testing of SFRC, because it is difficult to carry out and interpret the results. In all cases, the number of fibres in the governing plane will be small and it could present a fibre orientation effect due to the method of manufacturing. The bending test

plots load-deflection (load-crack mouth open displacement) relation, out of which stress-crack width (stress-strain) can be derived. Nominal values of the material properties can be determined by the results of 3-point bending test on a notched beam according to EN 14651[15] (Figure 2.9).

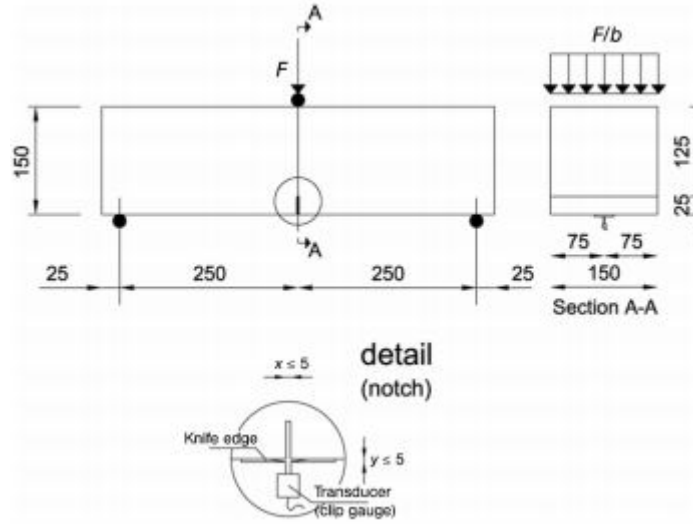


**Figure 2.9:** 3-point bending test, set up required by EN 14651

The deformation, as said, is generally expressed in terms of Crack Mouth Opening Displacement (CMOD), the values of residual flexural tensile strength which corresponds to certain CMOD<sub>j</sub> (residual flexural tensile strength corresponding to CMOD<sub>j</sub> ( $f_{R,j}$ )) could be estimated via F-CMOD relationship, as follows

$$f_{R,j} = \frac{3F_j l}{2bh_{sp}^2} \quad (2.9)$$

The residual flexural strengths ( $f_{r,j}$ ) of paramount importance are those which corresponds to CMOD=0.5mm (flexural residual strength CMOD=0.5mm ( $f_{R1k}$ )) and CMOD=2.5mm (flexural residual strength CMOD=2.5mm ( $f_{R3k}$ )) due to the requirement of these values for the calculation of the material constitutive law (Figure 2.10).

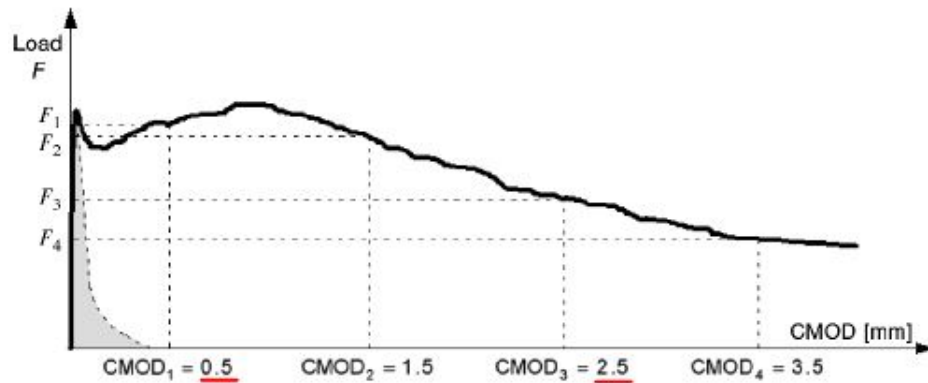


Figure 2.10: Typical load F-CMOD curve for plain concrete and FRC

### Linear model

The elastic linear model takes into account 2 reference values, namely serviceability flexural residual strength ( $f_{Fts}$ ) and  $f_{Ftu}$  which could be estimated by means of  $f_{R1k}$  and  $f_{R3k}$ , respectively (see equations below).

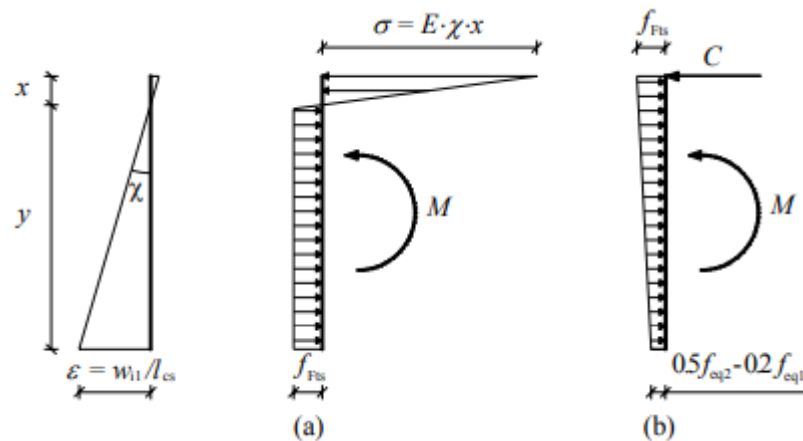


Figure 2.11: Stress diagrams for the determination of the residual tensile strength  $f_{Fts}$ (a) and  $f_{Ftu}$  (b) for linear model, respectively

$$f_{Fts} = 0.45 \cdot f_{R1} \tag{2.10}$$

$$f_{Ftu} = f_{Fts} - \frac{w_u}{CMOD_3} \cdot (f_{Fts} - 0.5 \cdot f_{R3} + 0.2 \cdot f_{R1}) \quad (2.11)$$

### Rigid-plastic model

The rigid-plastic model considers only one reference value which is based on the ultimate behaviour ( $f_{Ftu}$ ). As it possible to appreciate in the Figure 2.12), the next assumption is proposed for the rigid-plastic model in question: the whole compressive force is concentrated in the top fibre of the section.

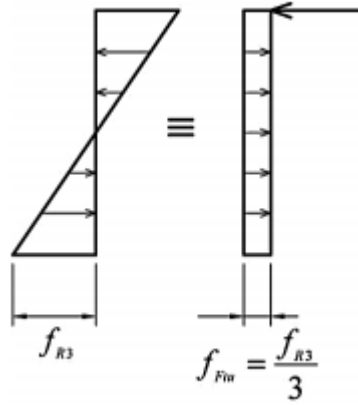


**Figure 2.12:** Rigid-plastic model

$$f_{Ftu} = \frac{f_{R3}}{3} \quad (2.12)$$

The nominal value of  $f_{Ftu}$  could be calculated taking into consideration the results of the 3-point bending test as it was stated previously, that has the following mathematical expression:

$$M_u = \frac{f_{R3} \cdot b \cdot h_{sp}^2}{6} = \frac{f_{Ftu} \cdot b \cdot h_{sp}^2}{2} \quad (2.13)$$

The Equation 2.13 refers to ULS, fixing the bending moment equilibrium and considering tensile stress constant. The diagram  $\sigma$ - $w$  in the

situation of post-cracking will be, respectively for rigid plastic and linear model, as in Figure 2.13.

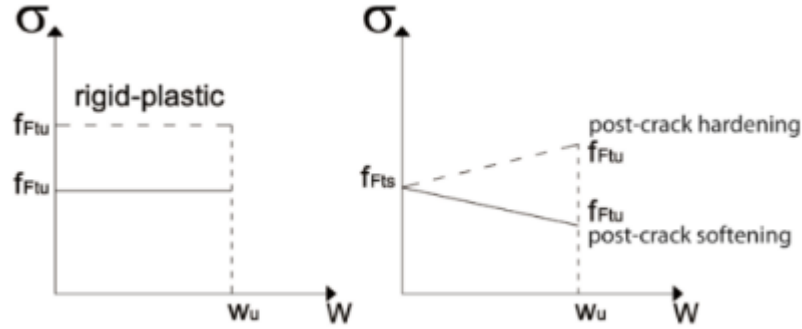


**Figure 2.13:** Simplified post-cracking constitutive laws: hardening (dashed line) and softening (continuous line)

## 2.4.5 Multilinear Model for FRC

The bending moment test, based on performances concrete, needs some mathematical equations in order to obtain  $\varepsilon$  and  $\sigma$ . In this work, it is studied the behaviour of a SFRC with softening and hardening behaviour. Stress-strain relation is based on the crack width depending by variation of  $l_{cs}$  of structural element. The deformation will be according to Equation 2.14 [14]:

$$\varepsilon = w/l_{cs} \quad (2.14)$$

In elements with OR,  $l_{cs}$  can be valuated as:

$$l_{cs} = \min\{s_{rm}, y\}$$

where  $y$  is the distance between the neutral axis ( $x_n$ ) and the tensile side of the cross section (Figure 2.11), neglecting tensile strength of SFRC. For the slab  $y=h$ , like unreinforced element or combined external forces (M-N). When the element is designed with OR,  $l_{cs}$  is calculated directly with the Equation 3.5 [14].

$$s_{rm} = l_{s,max} = k \cdot c + \frac{1}{4} \cdot \frac{(f_{ctm} - f_{Ftsm})}{\tau_{bm}} \cdot \frac{\phi_s}{\rho_{s,ef}} \quad (2.15)$$

It has been used the mean values of strain and strength, calculated experimentally, not only because the tensioned concrete hardening behaviour

shows a widespread cracking, but also because the case study of flat slab, that will be explained in the Chapter 6..... The mean values of stress and strength ( $f_{ctm}, f_{Ftsm}, f_{R3m}, f_{R1m}, f_{Ftu} \dots$ ) and 2% fibre ultimate strain ( $\epsilon_{Fu}$ ). In the particular case of fibres values, the mean stress is calculated, according the fib MC10 [14], dividing the characteristic value for 0.7.

$$f_{Xm} = \frac{f_{Xk}}{0.7} \quad (2.16)$$

The relationship between stress-strain, as described, depends by the model taken in account and also the tensioned concrete behaviour: hardening or softening. The following tables and images show the stress-strain diagram and the main points coordinates for their construction. For softening behaviour and elastic linear model, see the Figure 2.14 and Table 2.3.

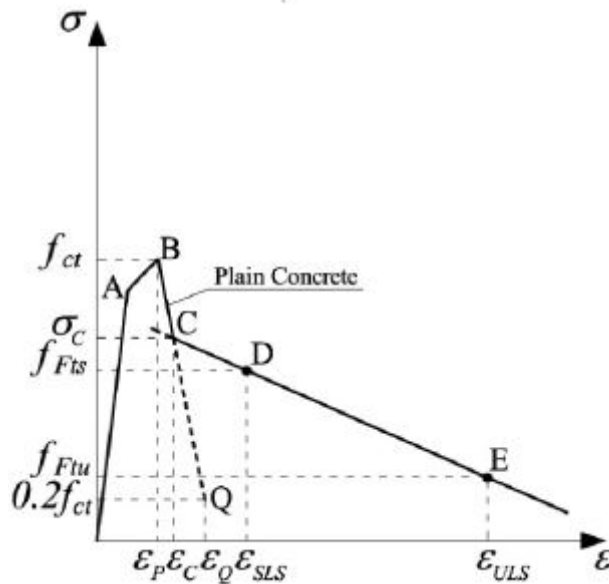


**Figure 2.14:** Stress-strain relation for softening behaviour of FRC

Point	Stress	Strain
B	$f_{ctm}$	$\varepsilon_P = f_{ctm}/E_{cm}$
C	intersection point between	BQ-DE
D	$f_{Fts}$	$\varepsilon_{SLS} = CMOD_1/l_{cs}$
E	$f_{Ftu}$	$\varepsilon_{ULS} = \min\{2\%; \min(\varepsilon_{Fu}, 2, 5/l_{cs})\}$
Q	$0.2 \cdot f_{ctm}$	$\varepsilon_Q = \frac{G_f}{f_{ctm} \cdot l_{cs}} + \left(\varepsilon_P - \frac{0.8 \cdot f_{ctm}}{E_c}\right)$

**Table 2.3:** Main points for trilinear tensioned concrete softening behaviour

The fracture energy of plain concrete ( $G_f$ ) is calculated, according to fib MC10 [14]:  $G_f = 73 \cdot f_{cm}^{0.18}$ . For hardening behaviour of SFRC and elastic linear model, see Figure 2.15 and Table 2.4.

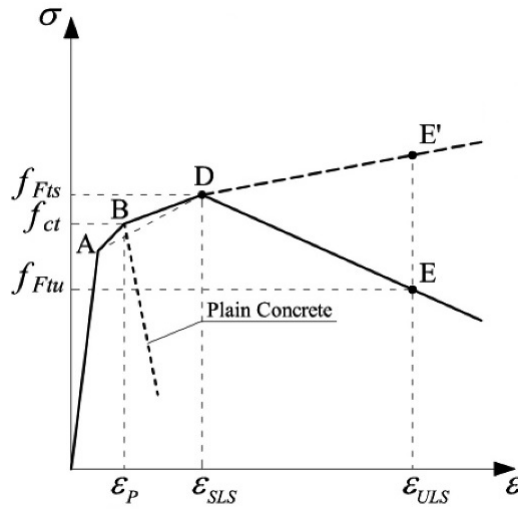


**Figure 2.15:** Stress-strain relationship for hardening behaviour [14]

Point	Stress	Strain
B	$f_{ctm}$	$\varepsilon_P = f_{ctm}/E_{cm}$
D	$f_{Fts}$	$\varepsilon_{SLS} = CMOD_1/l_{cs}$
E	$f_{Ftu}$	$\varepsilon_{ULS} = \min\{2\%; \min(\varepsilon_{Fu}, 2, 5/l_{cs})\}$
Q	$0.2 \cdot f_{ctm}$	$\varepsilon_Q = \frac{G_f}{f_{ctm} \cdot l_{cs}} + \left( \varepsilon_P - \frac{0.8 \cdot f_{ctm}}{E_c} \right)$

**Table 2.4:** Main points for trilinear tensioned concrete hardening behaviour

For rigid plastic model the stress value of tensioned concrete is constant and could be equal to  $f_{Fts}$  or  $f_{Ftu}$ , depending by ULS or SLS.

Depending by ULS or SLS case study, also, the diagram will be scaled according to partial safety factors. In the Table 2.5 a summary of them.

$\gamma$	ULS	SLS
Steel	1.15	1
Fibre	1.5	1
Concrete	1.5	1

**Table 2.5:** Safety factors

### 2.4.6 Classification of fibres

To classify a SFRC is considered the ratio  $f_{R3k}/f_{R1k}$  associated to a letter from *a* to *e*. In particular:

- *a* if the ratio is [0.5 – 0.7];
- *b* if the ratio is [0.7 – 0.9];
- *c* if the ratio is [0.9 – 1.1];
- *d* if the ratio is [1.1 – 1.3];
- *e* if the ratio is  $\leq 1.3$ .

The following Table 2.7 and Figure 2.16 show the coordinates for the construction of some examples of sections with different properties. Below are 4 examples (Table 2.6).

	Code	$f_{ck}$ [Mpa]	$f_{R3k}$ [Mpa]	ratio [-]	$f_{R1k}$ [Mpa]	$A_{top}$ [mm <sup>2</sup> ]	$A_{bot}$ [mm <sup>2</sup> ]	Hardening/ Softening
1	FRC50-5.3b	50	4	0.75	5.3	0	0	H
2	FRC50-3c	50	3	1	3	360	842	H
3	FRC40-10.7b	40	8	0.75	10.7	0	0	S
4	FRC40-10a	40	5	0.5	10	360	842	S

**Table 2.6:** Examples

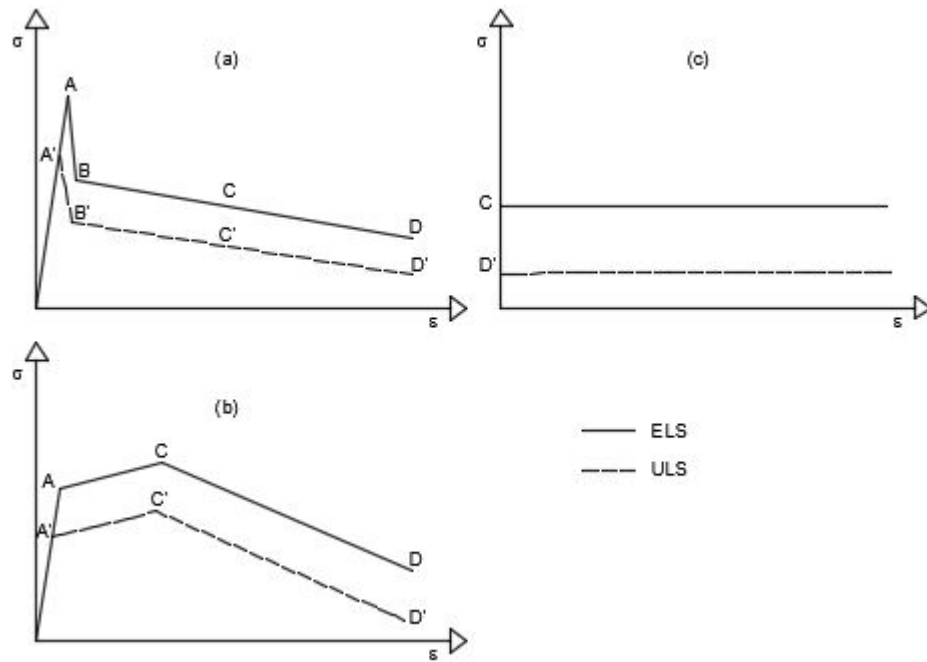


**Figure 2.16:** Drawing of the coordinates:(a) Linear elastic model hardening behaviour, (b) Linear elastic model softening behaviour (c) Rigid plastic model

		ELS				ULS			
		A	B	C	D	A'	B'	C'	D'
1	$\epsilon$	0.0001	0.00014	0.0025	0.0125	0.00007	0.00016	0.0025	0.0125
	$\sigma$	4.07	2.74	2.4	0.93	2.71	1.83	1.60	0.62
2	$\epsilon$	0.0001	0.00022	0.0029	0.0149	0.00007	0.00029	0.003	0.015
	$\sigma$	4.07	1.45	1.35	0.90	2.71	0.97	0.90	0.60
3	$\epsilon$	0.0001	=A	0.0025	0.0125	0.00006	=A'	0.0025	0.0125
	$\sigma$	3.51	=A	4.80	1.87	2.34	=A'	3.20	1.24
4	$\epsilon$	0.0001	=A	0.0025	0.0125	0.00006	=A'	0.0025	0.0125
	$\sigma$	3.51	=A	4.50	0.50	2.34	=A'	3.00	0.33

**Table 2.7:** Values coordinates  $\sigma - \epsilon$



## Chapter 3

# Control crack

The main beneficial effect offered by the fibres is that of improving the ductility of the conglomerate in the phase following the initiation of the cracking phenomenon. In fact, since the elongation at fracture of all the fibres is about 2-3 orders of magnitude higher than the deformation at fracture of the concrete matrix, the conglomerate crisis occurs long before the fibres can break. Therefore, the fibres reduce the brittle behaviour of the cement matrix, which would otherwise tend to collapse after the first cracks have occurred. Once the deformation of the first cracking has been reached, the fibre-reinforced concrete has an elasto-plastic behaviour (ductile behaviour) in the post-flexure phase, i.e. it can still withstand loads after the first cracks have occurred. The presence of fibers therefore increases the toughness (ability of the concrete to withstand the advancement of cracks) of the concrete. In fact, the presence of fibres in the cement matrix prevents the propagation of cracks, which are generated in the concrete due to the onset of tensile stresses (due to shrinkage and/or external loads) which, even at low levels of intensity, exceed the tensile strength of the mix, causing the fracture of the cement matrix. At high fibre dosages (indicatively for fibre volumes of more than 2%), the fibres also significantly improve the strength of the concrete a pure traction: the post-cracking behaviour of tensile concrete is influenced by the effective stitching action exerted by the fibres, which involves the progressive triggering of a multiplicity of cracks until a tension of collapse is reached which is greater than that which caused the appearance of the first injury. With low fibre dosages (indicatively for fibre volumes of less than 2%), concrete, on the other hand, after the crack has been triggered, is able to withstand tensile stresses provided that these are lower than those that caused the cracking of the cement matrix; Fibres do not bring

any significant advantage in terms of compressive strength of concrete and are not able to significantly influence the compressive modulus of elasticity. The action of the fibers manifests itself only after the cracking of the concrete. In fact, after the formation of the first cracks in the cement matrix, the fibres are activated, assuming a sewing effect of the openings, creating a sort of crack-bridging bridge between the edges of the cracks themselves. This leads to a reduction in the crack width and, thanks to the stitching effect, the fibre guarantees the concrete a residual tensile strength even in the post-peak phase since this allows the transfer of the tensile forces from one edge of the lesion to another; this phenomenon is often referred to in the literature as tension-softening. In addition, the addition of fibers leads to a substantial improvement in the adhesion between concrete and surrounding bars (tension stiffening). The combination of these two effects (the stiffening effect of tension stiffening and the post-peak stress transmission effect of tension-softening) leads to a substantial change in the structural behaviour of reinforced concrete elements, especially as regards cracking, the distance between cracks and their width. At sight, a normal concrete, once cracked, has wide and localized openings while the FRC one is characterized by widespread cracks and smaller widths, which certainly determines a benefit for the durability of the material as it reduces the risk of attack by aggressive weathering agents. Increasing the fibre content increases the tensile strength of the concrete during the post-peak phase; at very high dosages, the evolution of the cracking phenomenon can also be blocked.

In this chapter the calculation models for the crack width are analysed, in particular, for ORC, SFRC and hybrid solutions (HRC).

### 3.1 Cracking model in ordinary reinforced concrete

The theoretical description of cracking in ordinary steel reinforcement concrete (ORC) is referred to tension tie, but the study can be generalised to bending element. As explained in literature [16], on the base of strut-tie theory of *Ritter-Mörsh*, a tensioned element remains in equilibrium and uncracked until the strain compatibility between steel and surrounding concrete is verified. After the material reaches the certain strain which depends on the mechanical properties of the concrete, crack concrete strain ( $\varepsilon_{cr}$ ) ( $= f_{ct}/E_c$ ) a first crack appears, reaching different phases, depending on load. In Fig-

ure 3.1 are shown all phases.

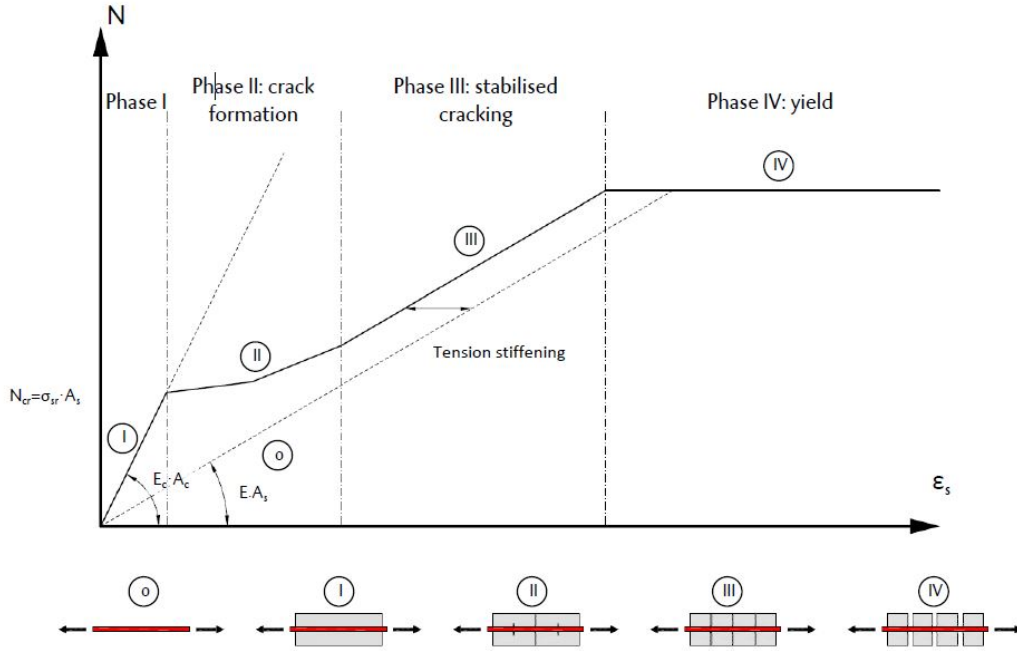


**Figure 3.1:** Tension-average steel strain in all phases [17]

The mathematical equation of Figure 3.1 could be appreciated in the Equation 3.1. An important aspect, for the quantification of crack width, is the stiffening of the section that, in Phase III, has a value between section cracked and homogenised stiffening.

$$N_{cr} = A_c(1 + \alpha_{E\rho_{s,ef}})f_{ct} \quad (3.1)$$

The corresponding cracking moment ( $M_{cr}$ ) can be computed by using Phase I hypothesis, like in tensile strength  $f_{ct}$  is reached in the tension surface, where section modulus of the element ( $W_I$ ) [16].

$$M_{cr} = f_{ct,fl} \cdot W_I \quad (3.2)$$

### 3.1.1 Cracking stages, transfer length, crack spacing

When the external force reaches the certain value  $N_{cr}$ , the first crack will occur at the place with the lowest tensile strength anywhere in the bar. In this phase it is possible to identify the transmission area of the concrete which will carry more of the tensile stress by increasing the distance of the crack, because of the bond between the reinforcing steel and the concrete.

That value is cited in Equation 3.5 for the definition of stress-strain trilinear model of tensioned concrete. For the conventionally reinforced concrete, the value of the transfer length ( $l_t$ ) is obtained by imposing equilibrium between cracked and the no-slip sections (see Figure 3.2, assuming Saint-Venant's principle: *the difference between the effects between the effects of two different but statically equivalent loads becomes very small at sufficiently large distances from the load*). It depends only on geometrical ratio (diameter steel bar ( $\phi_s$ ) and effective reinforcement ratio ( $= A_s/A_{c,ef}$ ) ( $\rho_{s,ef}$ )) and the mechanical properties of material ( $f_{ct}$  and mean bond strength between steel and concrete ( $\tau_{bm}$ )). That can be assumed equal to mean distance value between cracks ( $s_{rm}$ ) and its maximum  $2 \cdot l_t$ .

$$s_{rm} = 2 \cdot l_t = 2 \cdot \frac{f_{ct}\phi_s}{4\tau_{bm}\rho_{s,ef}} \quad (3.3)$$

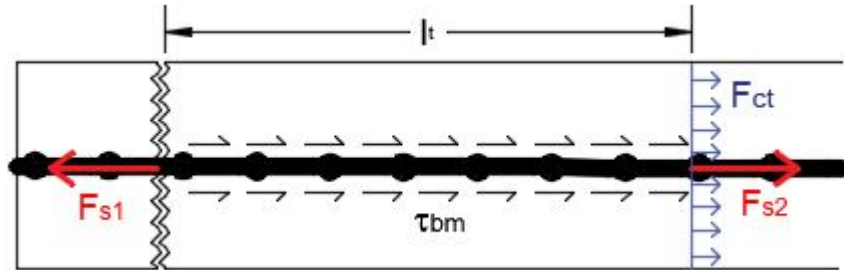


Figure 3.2: Transfer length [17]

However, the Equation 3.4 have to take in account two particular aspects.

1. Difference between bending moment and axil force;
2. Cover contribution

As Equation 3.4 shows, Concrete cover (multiplied by certify coefficient,  $\kappa \cdot c$ ) increases the value of  $l_t$ . That's because the first one considers in bending the amount of stress needed to crack concrete that is half of uniform stress throughout entire section transferred by  $l_t$ ; this *strain/stress gradient* causes the increase the crack width from the position of bars to the surfaces [18] and it can be assumed 0.125 for bending, 0.250 for axial [7]; the second one it is because according to A.W. Beeby [19] there is a dependence between concrete cover ( $c$ ) and crack width based on experimental evidence and in particular a *stress lag* increases the distance at which the cracks appears at the surface. Considering the above described statements, the value of mean crack spacing could be evaluated by means of the next equation:

$$s_{rm} = \kappa \cdot c + 2 \cdot l_t = \kappa \cdot c + 2 \cdot \frac{f_{ct} \phi_s}{4 \tau_{bm} \rho_{s,ef}} \quad (3.4)$$

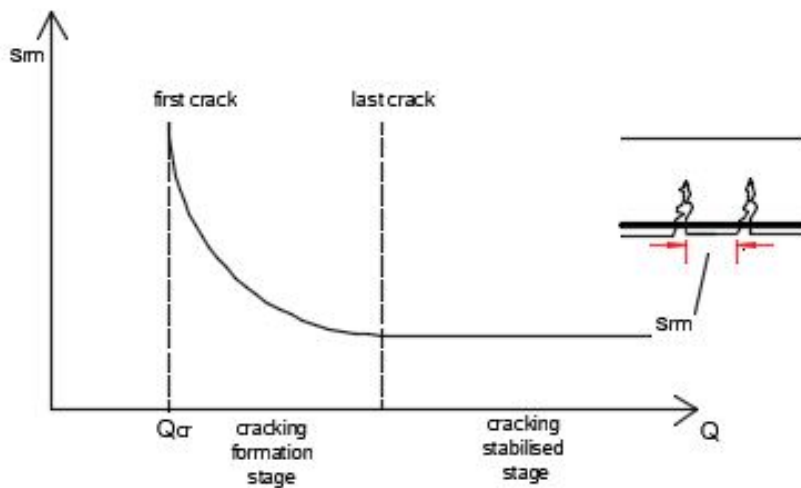


**Figure 3.3:** Crack spacing - Load

At the place of the crack the stress in the concrete will reduce to zero and the stress in the reinforcing steel increase. The reinforcing steel is carrying the tensile force. In an intermediate point between a crack and the next one, tension in concrete increases due to the force transmitted by bars through bond, until it drop to zero again at the crack. For the same reason, the tensile stresses reaches its maximum at the crack.

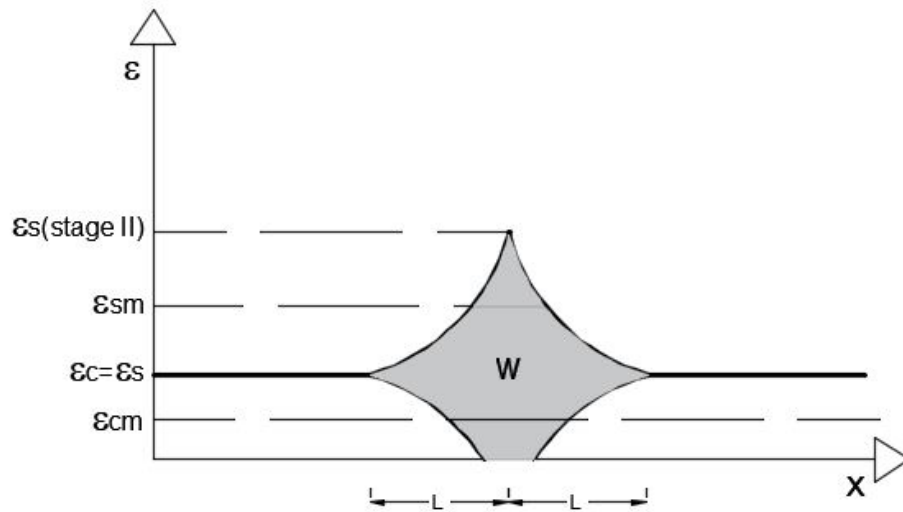


Figure 3.4: Detail of a crack

## 3.2 Cracking in FRC

The incorporation of fibres to the concrete mix leads to the next benefits once the element, subjected to the tensile stresses, is cracked:

1. crack spacing reduces;
2. concrete mean strain increases;
3. steel mean strain decreases for the same tensile stresses in comparison with the ORC.

In order to evaluate the contribution of fibres to the crack width control, firstly, the material should be studied by means of certain tests. The most common test to characterize the SFRC, as it was stated previously, is 3-point bending test.

### 3.2.1 Transfer length and crack spacing

In presence of SFRC, the  $l_t$  reduces due to the bridging effect that fibres provide in the crack (Figure 3.5).

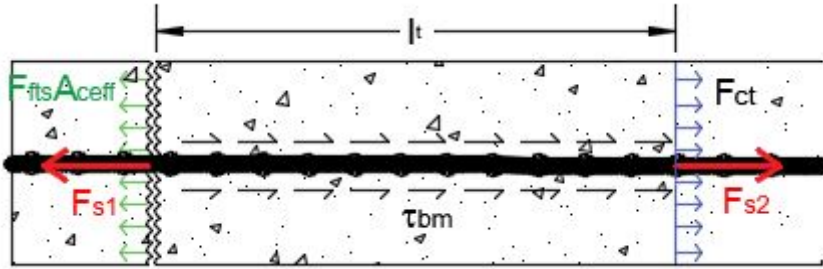


Figure 3.5: Transfer length in FRC [17]

Considering the contribution of fibres in concrete mix, fib MC10 provides the Equation 3.5 in order to evaluate the mean crack spacing. As it possible to note, in contrast to Figure 3.6, the concrete keeps having certain tensile strength even once it is cracked:

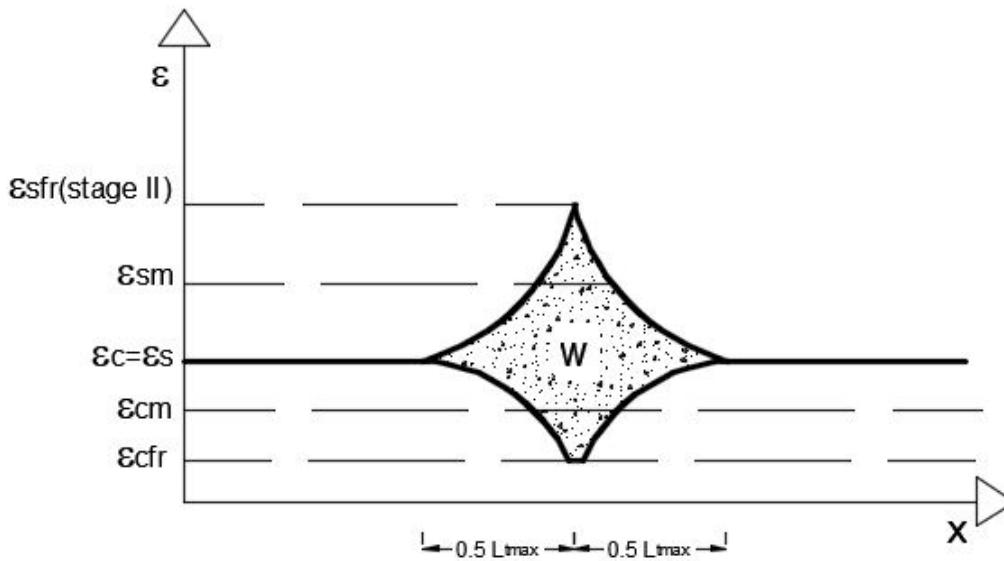


Figure 3.6: Strains around FRC crack

The difference  $(f_{ctm} - f_{Fts})$  in the equation (3.3):

$$s_{rm} = l_{s,max} = k \cdot c + \frac{1}{4} \cdot \frac{(f_{ctm} - f_{Ftsm})}{\tau_{bm}} \cdot \frac{\phi_s}{\rho_{s,ef}} \quad (3.5)$$

### 3.3 Mean steel strain

As shown in Groli [17], some tension is taken by fibres at the crack, mean steel strain is reduced. Contrarily to the case of ORC, it is difficult to provide an closed expression to obtain the tensile stress of the steel in presence of tensile strength along the all section. It can be founded by means of iterative procedure, explained in the next chapter. This is what is recommended in RILEM guidelines [5] and fib MC10 [14]. The mentioned reduction of the tensile stresses in the conventional reinforcement could be appreciated in detail in the Figure 3.7:

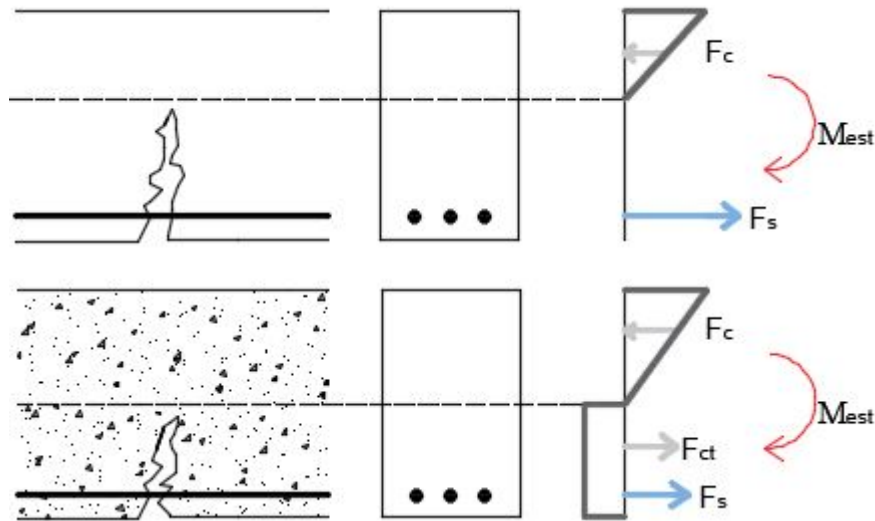


**Figure 3.7:** Stress steel reduction due to presence fibers

In numerical terms, according to Groli, for  $f_{Fts} = 2$  Mpa and  $\rho_{s,ef} = 1\%$  the improvement will be of 0.1%, in terms of steel strain. Since the serviceability ranges for steel strain between 0.1% and 0.15%, this is a considerable improvement. As a summary [20], the main differences are:

1. Transmission length: the post-cracking tensile strength provides a reduction of transmission length, this reduction is explainable; less force has to be transmitted by bond between the concrete and the reinforcing steel;
2. As a result of contribution of the steel fibres, the stresses in the rein-

forcing steel reduces. Less stress in the reinforcing steel  $\sigma_s$  provide the in a lower elongation of reinforcing steel and the crack width will be also reduce:

3. The stress in the reinforcement during the crack formation stage reduces as a result of the contribution of fibres. The tensile force has been transmitted partly by the steel fibres.

### 3.4 Estimation of crack width for FRC

Crack form in reinforced concrete is due to the slip between concrete and reinforcing steel. This differential slip, integrated over the distance between two point of zero slip provides the crack width opening (Equation 3.6).

$$w_m = \int_0^l (\varepsilon_s(x) - \varepsilon_c(x))dx = (\varepsilon_{sm} - \varepsilon_{cm}) \cdot l_t \quad (3.6)$$

The procedure to evaluate the strain which affects on the crack width is, in general terms, the same for both types of concrete and could be appreciated in the Equation 3.7. It is important to highlight that within the study in question, the contribution of the shrinkage phenomena was neglected. fib MC10 [7]

$$\varepsilon_{sm} - \varepsilon_{cm} - \varepsilon_{cs} = \frac{\sigma_s - \beta \cdot \varepsilon_{sr}}{E_s} - \eta_r \cdot \varepsilon_{sh} \quad (3.7)$$

However, the transfer length should be calculated with the adjustments on the basis of the type of concrete. Having this in mind, the crack width is to be calculated, in accordance with fib MC10 [14], in the following way. For ORC:

$$w = \kappa \cdot c + \frac{1}{4} \frac{f_{ctm}}{\tau_{bm}} \frac{\phi_s}{\rho_{s,ef}} \frac{1}{E_s} (\sigma_s - \sigma_{sr} \cdot \beta) \quad (3.8)$$

For SFRC:

$$w = \kappa \cdot c + \frac{1}{4} \frac{f_{ctm} - f_{Fts}}{\tau_{bm}} \frac{\phi_s}{\rho_{s,ef}} \frac{1}{E_s} (\sigma_s - \sigma_{sr} \cdot \beta) \quad (3.9)$$

Where  $\beta$  [7] is an empirical coefficient to assess the mean strain over  $l_{cs}$  depending on the type of loading;  $\sigma_{sr}$  has been calculated as the steel stress at  $M_{cr}$ . The value of  $\sigma_s$  will be discussed on the next section. In the case study, for the crack width calculation has been utilised the general formula (Equation 3.10) of EHE08 [9], because it is more restrictive since the contribution of the fiber is considered implicitly compared to fib MC10. In fact,

thanks to the addition of fibres, the stresses in the reinforcement will have lower values.

$$w_k = \beta \cdot s_{rm} \cdot \varepsilon_{sm} \quad (3.10)$$

where:

$s_{rm}$  is calculated according to the Equation 3.11.

$$s_{rm} = 2c + 0.2s + 0.4k_1 \frac{\phi_s \cdot A_{c,eff}}{A_s} \quad (3.11)$$

$s$  is the distance between bars (max  $15\phi_s$ );

$k_1$  is a coefficient which is equal to 0.125 in case of bending and 0.250 if the element is subjected to tension;

$A_{c,eff}$  is the concrete area surrounding the bars that contribute to the closure of the crack. ( $h/4$  in the case of a beam).

$\varepsilon_{sm}$  is the mean elongation bars, considering the concrete contribute, is which could be calculated in accordance with the Equation 3.12

$$\varepsilon_{sm} = \frac{\sigma_s}{E_s} \left[ 1 - k_2 \left( \frac{\sigma_{sr}}{\sigma_s} \right) \right]^2 \geq 0.4 \cdot \frac{\sigma_s}{E_s} \quad (3.12)$$

$k_2$  is a coefficient equal to 1 for non-repeated loads and 0.5 for repeated ones.

## Chapter 4

# Definition of M-N envelopes

In order to perform a verification at ULS and SLS, it could be useful to define M-N envelopes. The verification or design of a structural element is performed by checking, in the most general case, that the point of coordinates Internal axial force ( $N_{est}$ ) and External bending moment ( $M_{est}$ ) is internal to the breaking domain of the section; the geometric place described, in a plane M-N, by the pairs of stresses M and N that bring the section in ultimate or service conditions. The assumptions considered are:

1. Hypothesis of planar section;
2. Concrete constitutive law: linear and non-linear for the compression, rigid-plastic and linear elastic for the tension ;
3. Steel constitutive law, as described in the 2nd chapter;
4. Plastic deformation both in tension and compression steel bars.

For the determination of the breaking domain it is followed a simplified procedure on the basis of the identification of 4 points under the following conditions of external forces and others intermediate for each domain.

1. Simple tension ( $M = 0, N > 0$ );
2. Simple compression ( $M = 0, N < 0$ );
3. Simple bending ( $M = M_{est}, N = 0$ );
4.  $M_{est}$  and  $N_{est} \neq 0$ .

## 4.1 M-N envelopes at ULS for FRC

In order to draw the M-N envelopes related to ULS of fibre-reinforced elements, the design compressive and tensile stresses are evaluated according to fib MC10. Nevertheless, the maximum tensile strain cannot exceed the value related to a maximum crack width  $w$  of 2.5 mm. Design value of compressive strength of concrete  $f_{cd}$ , depends on safety factor (Table 2.5) and the time  $t$  considered with long-term load application coefficient ( $\alpha_{cc}$ ) equal to 1.

$$f_{cd} = \frac{f_{ck} \cdot \alpha_{cc}}{\gamma_c} \quad (4.1)$$

The design value of tensile strength of concrete is, according to the the two models explained in fib MC10. In the Figure 4.1 can be compared the M-N envelopes at ULS, for an element with  $h=200\text{mm}$ , FRC40-4c not reinforced.

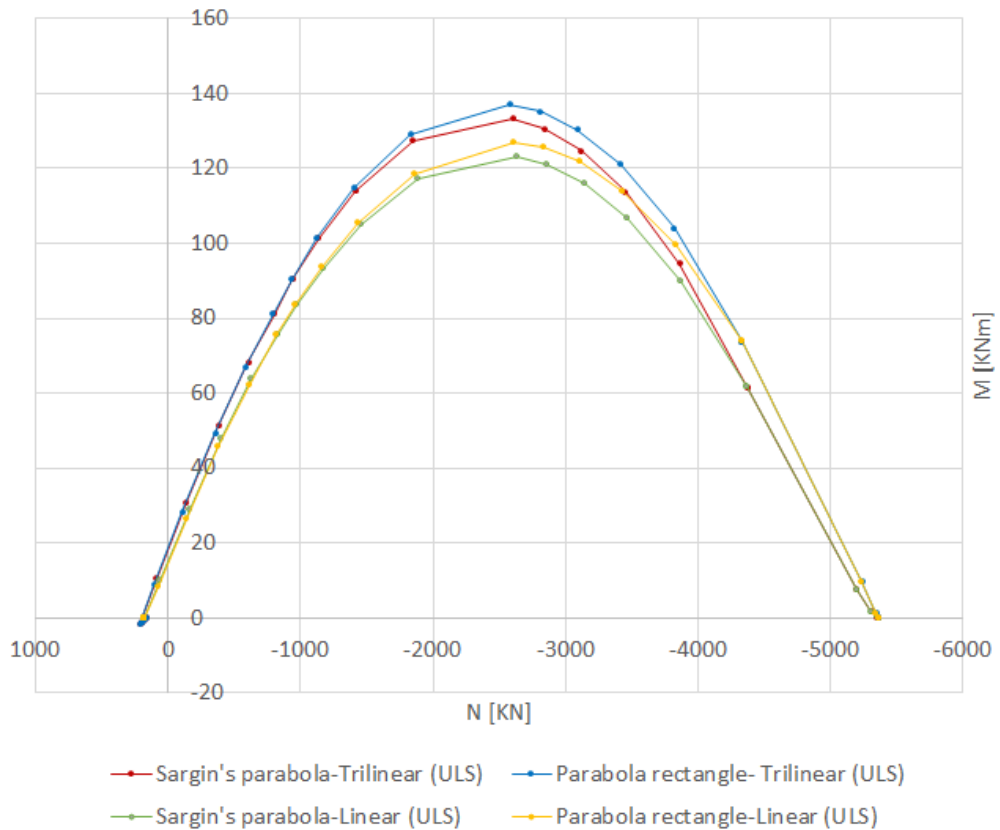


**Figure 4.1:** M-N envelopes for different constitutive laws at ULS

Figure 4.2 presents the behaviour of the elements with the same mechanical properties (FRC40-4c) and different depths:

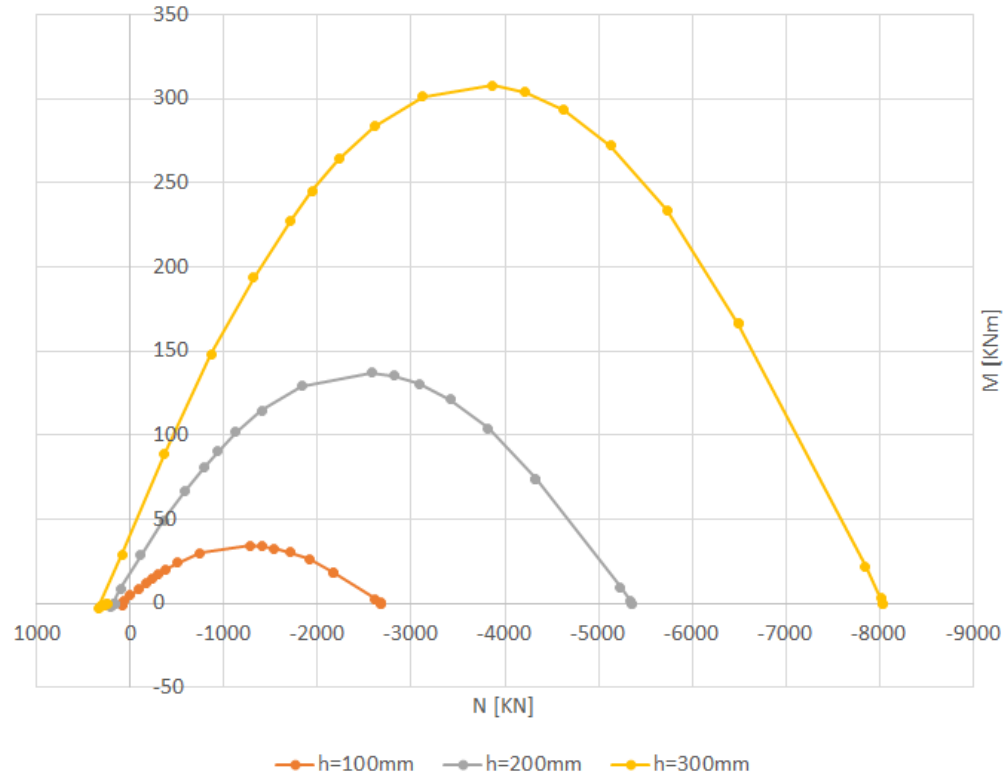


**Figure 4.2:** M-N envelopes for different sectional depths [mm] at ULS (Sargin's parabola-linear elastic model)

## 4.2 M-N envelopes at SLS for FRC

At SLS, the M-N envelope could be calculated according to the required crack width ( $w_d$ ). In the study in question, the linear elastic model for concrete in tension has been applied. In the Figure 4.3 and 4.4 could be compared the M-N envelopes and constitutive laws at SLS, for the element (h=300mm) with FRC40-4c at different  $w_d$ :

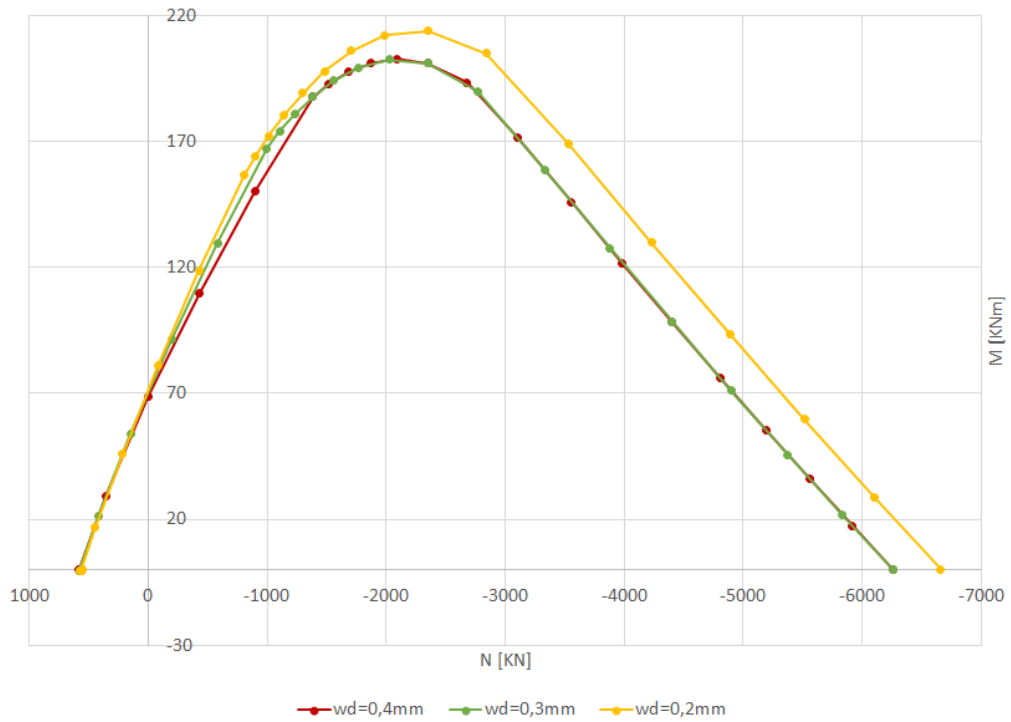


**Figure 4.3:** M-N envelopes for different  $w_d$  [mm] at SLS (Sargin’s parabola-linear elastic model)

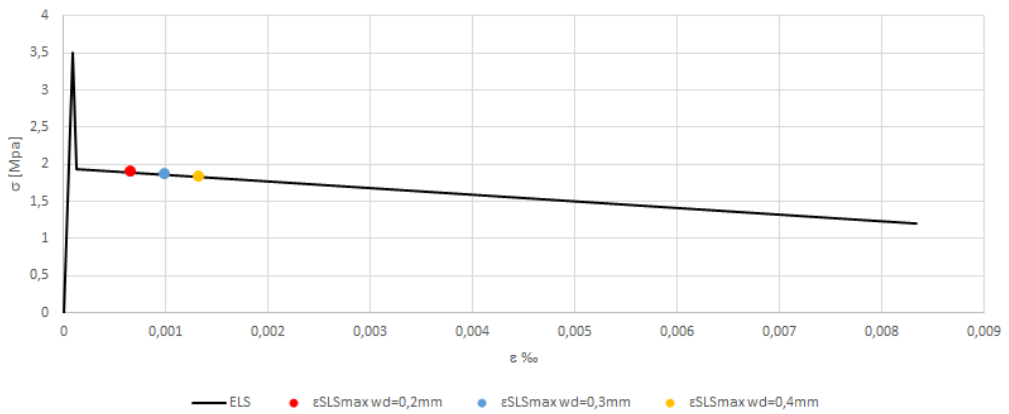


**Figure 4.4:** Limitation for elastic linear model at SLS for different  $w_d$

### 4.3 Comparison of the results at ULS and SLS

The comparison of the the two model appears in the Figure 4.6.

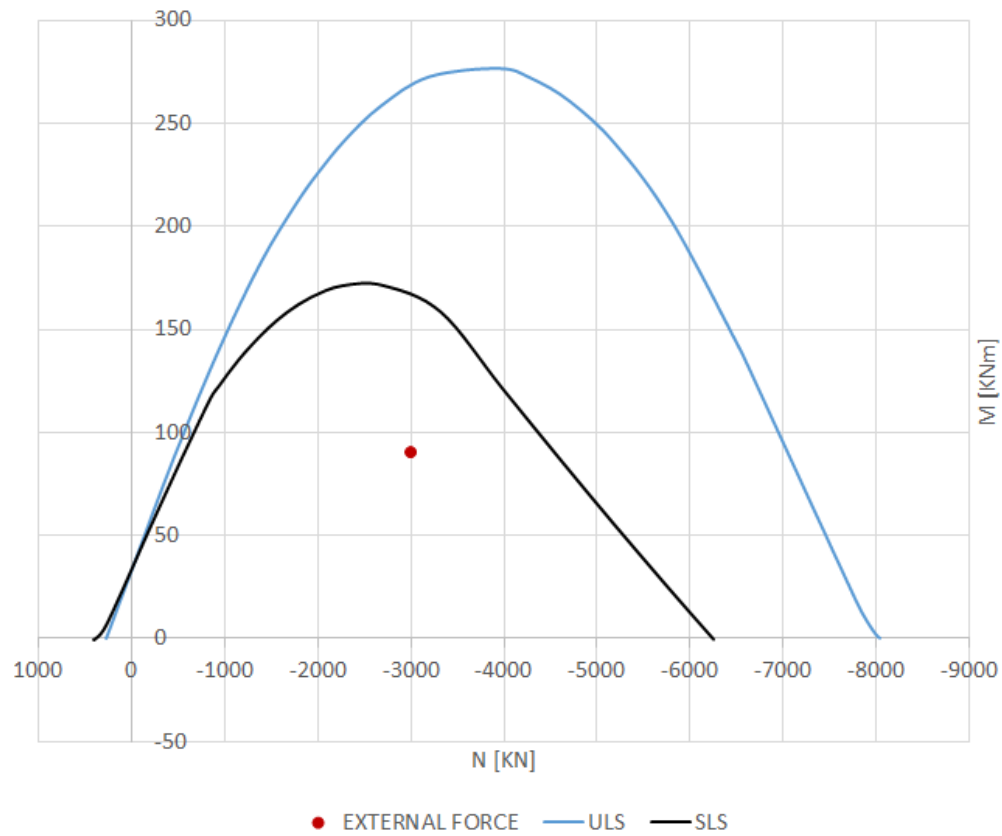


**Figure 4.5:** FRC40-4c h=300mm wd=0.3. Comparison ULS-SLS

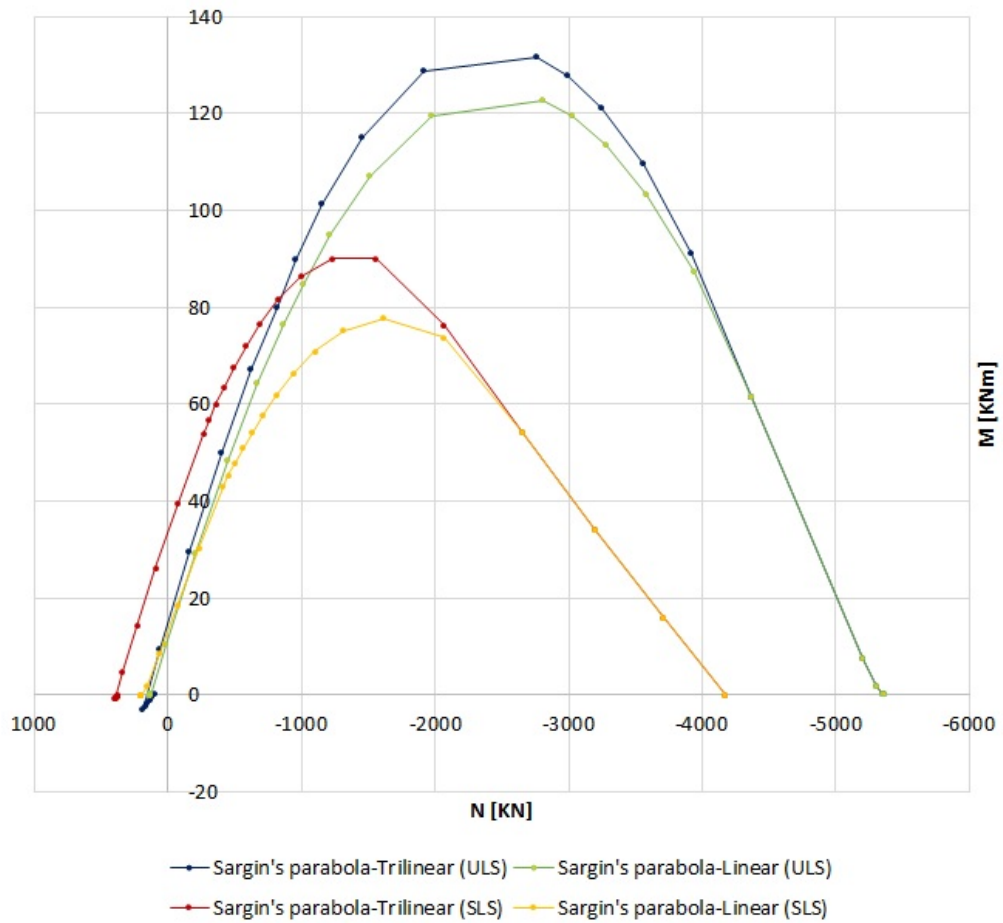


**Figure 4.6:** FRC40-3c h=300mm wd=0.4. Comparison models

The rigid plastic model appears more restrictive. This can be seen more in the left part of the diagram where the contribution of the tensioned concrete is more relevant.

## 4.4 Effect of fibres on behaviour of the material (M-N envelope)

Comparing the M-N envelopes at ULS for different reinforcement solutions it is possible to note the benefits of fibre incorporation to the concrete mix. Figure 4.7 demonstrates the behaviour of the element with the established

geometrical parameters (  $b = 1000\text{mm}$ ,  $h = 300\text{mm}$ ) for different types of the reinforcement:

1. Plain concrete;
2. Conventional reinforcement:  $4 \phi_s 16$  on top and 2 on bottom;
3. SFRC40-4c;
4. The hybrid solution which comprises both types of reinforcement (see 2 and 3).

Looking to the left part of diagram, where it is possible to appreciate the contribution of fibres to the tensile strength of the material. As it was described in Chapter 2, the presence of fibres does not affect on the compression strength. Obviously, the performance of a SFRC depend on the fibre type. In the Figure 4.8 a comparison between FRC40-4c and FRC40-6b could be studied.

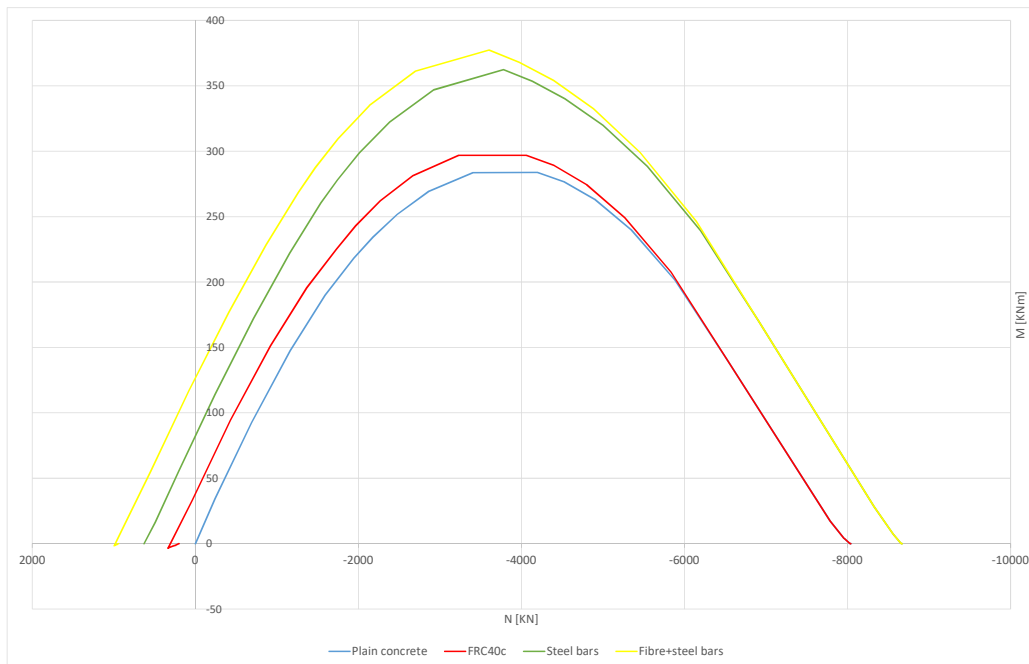


**Figure 4.7:** M-N envelopes for plain concrete, FRC, ordinary reinforced concrete and mix solution at ULS

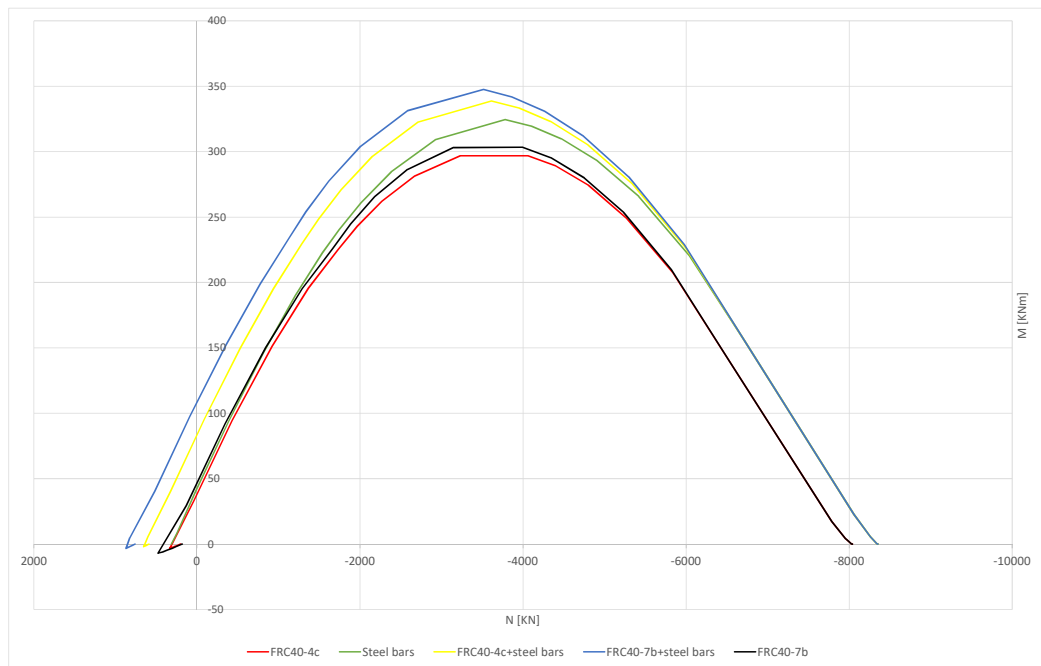


**Figure 4.8:** M-N envelopes for FRC40-6b and 4c with and without ordinary reinforcement

# Chapter 5

## Case study

Herein, the design procedure of flat slabs will be discussed, taking into consideration different types of reinforcement and, most importantly, the permitted crack width. The essential task of the chapter (and the thesis) is to find the best hybrid solution in terms of the amount of required steel for certain geometry and applied loads. It should be highlighted that the geometry of structure and the reference curve for different options of hybrid solutions has been taken from the Sutera's thesis [21] where the optimisation study of HRC for the flat slabs at ULS was carried out.

### 5.1 Model definition: flat slab

Flat slab's dimension and the material properties are arbitrarily set. For the case study it has been defined a slab with 4 spans in both directions which is supported by 25 columns placed at a distance (axis-to-axis) of 6 meters. The dimensions of mentioned columns in XY plane are 0.3 x 0.3 meters. The choice of the slab thickness ( $t$ ) has been done in order to limit the slab slenderness ( $t/L$ =thickness/span length) in the range:  $1/35 \leq t/L \leq 1/25$ . In this way the behaviour of the slab can be classified as that of a *thin plate*. Thin plates have such a flexural stiffness that they carry the two-dimensional load distributions mainly through bending moments, torques and shear in a manner similar to the beams. Considering the abovementioned range, the depth of the slab was established of 200 mm.. The material properties are: Steel B500C and concrete C50/60. A summarise of all proprieties could be found in the Table 5.1. The geometry is showed in the Figure 5.1.

Sections		Concrete C 50/60		Steel B500C	
b	1000 mm	fck	50 [Mpa]	fyk	500 [Mpa]
h	200 mm	fctm	4.07 [Mpa]	$\varepsilon_{su}$	0.01
c	30 mm	Ecm	38.6 [Gpa]	Es	210 [Gpa]
Panel	6x6m	$\alpha$	1		
Pillars	0.3x0.3 m				

Table 5.1: Model properties

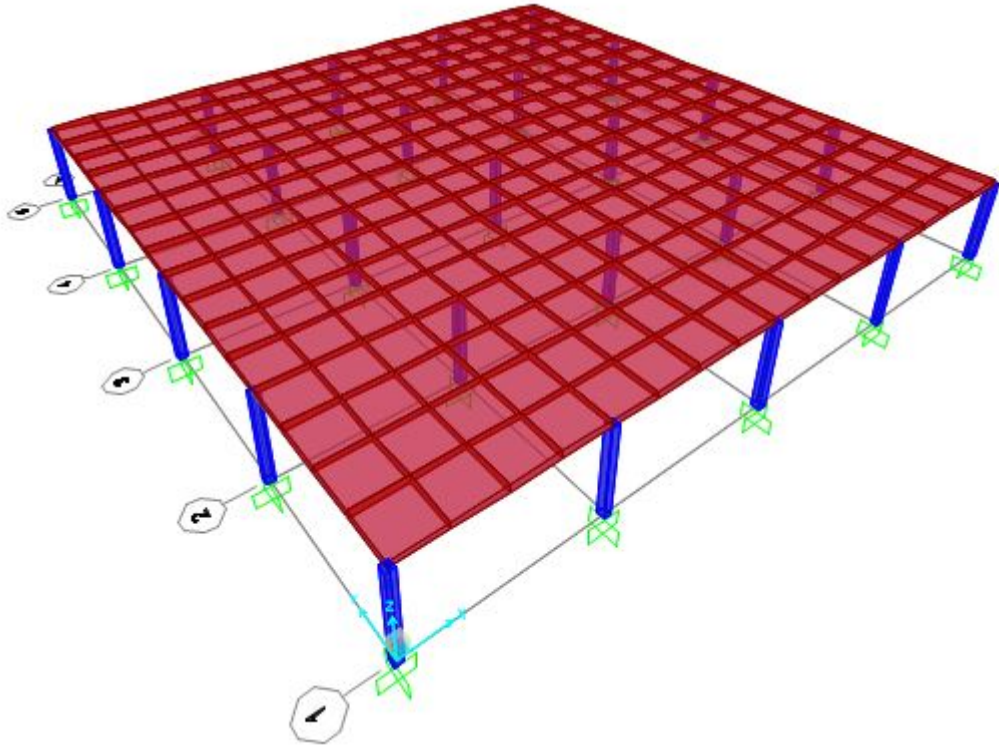


Figure 5.1: Model geometry

## 5.2 Hybrid Solution for flat slabs at ULS

### 5.2.1 Plastic analysis and Yield-Line Theory

The design moment at ULS of the studied slab was carried out by the Yield-Lines Theory in accordance with ACI 544.6R-15 [8]. That theory is a practical method for the plastic analysis which is based on *upper bond (kinematic) methods*. The Sutura's study [21] focus on the plastic analysis because it is an ultimate load analysis which, also, permits to appreciate certain ductility of the structure (provided, inter alia, by fibres). However, it needs a verification at SLS, in order to evaluate the crack widths which is of a paramount importance at the limit state in question. However, firstly, the brief explication of Sutura's approach in the thesis and the following results are presented below due to the requirement of the reference to the achieved results for hybrid solution at ULS. As it was stated above, the Yield Line Method was applied in order to evaluate how the moments were distributed throughout the slab. For this purpose, the next procedure should have been carried out:

1. Identification of *collapse mechanisms* and Yield Lines;
2. Application of the *principle of virtual works* in order to calculate the *external work*, due to the total load on the slab times the average displacement it moves through, and the *internal work*, due to the moment capacity of the yield line times the rotation it moves through along the length. More precise description of this step you can take in the "Practical Yield Line Design";
3. Equalisation of internal and external work and calculation of the *ultimate collapse load*.

Regarding the collapse mechanism, for elevated flat slab, according to ACI 554.6R-15 [8], the dominant failure mode is to be produced by the uniformly distributed load, with crack patterns that are characterised in two simplified mechanisms, as shown in Figure 5.2.

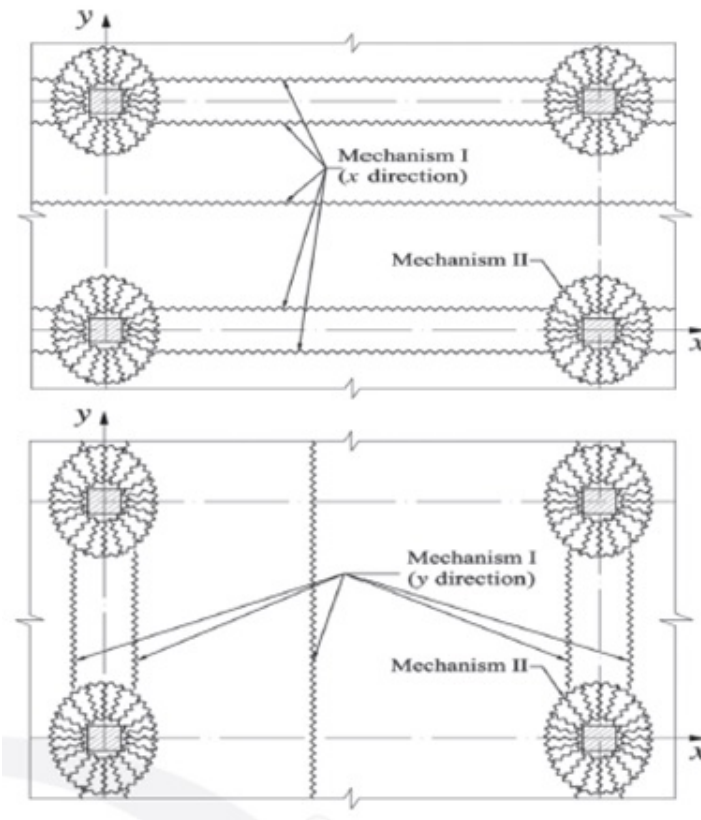


**Figure 5.2:** Collapse mechanisms for flat slab [8]

1. Global failure: positive and negative moment yield lines with the negative yield line forming along the axis of rotation passing over a line of the columns.
2. Local failure: negative yield lines emanate from the column and a positive circumferential yield line forms at the bottom of the cone shaped surface.

### Design arrangement of steel reinforcement

The positioning of reinforcement follows the criteria used in the Practical Yield Line Design [22]. According to Yield Line principles, the moment resistant given by top steel could be concentrated over only part of the whole span: around the column, with the improvement of resistant to local and

Location of column	Reinforcement concentrated in the area of dimensions	
	x (or y)	y (or x)
Internal	0.5 L	0.5 L
Edge	0.5 L	(0.2 L+E.D.)
Corner	(0.2 L+E.D.)	(0.2 L+E.D.)

**Table 5.2:** Top reinforcement distribution (E.D.= edge distance is the centerline of the column to the edge of slab)

punching failure and where the bending moment reaches the peak. The common concentration of top reinforcement follows the scheme in the Figure 5.3 and Table 5.2.

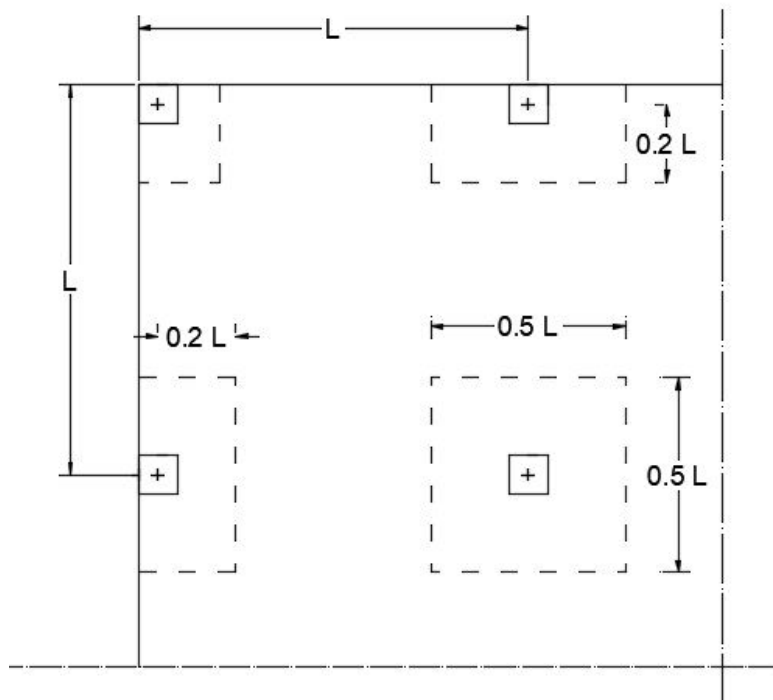


**Figure 5.3:** Top reinforcement distribution

The bottom reinforcement is positioned regularly over the whole slab, without curtailment, because it is assumed a constant moment along the whole length of yields lines.

### 5.2.2 Optimization of hybrid reinforcement for flat slabs

Within Sutura's study, the optimal amount of steel (fibre + conventional rebars) has been analysed for the flat slabs at ULS. It should be mentioned, that the hybrid solutions were compared with conventional one and the one which contained only fibres. Following the explained approach, the optimisation was carried out for different content of fibres ( $kg/m^3$ ) which, in turn, affected on the tensile strength. . In particular, the relation fibre content / residual tensile strength was taken from study which was carried out by the research group in the University of Brescia (Table 5.3) [23]. For greater clarity, each solution will be identified with a code + (int) or (ext) for internal or external panel:

- ORC- $\rho_s$  for the Ordinary Reinforced Concrete that provides only steel bars;
- HRC $f_{R3k}$ - $\rho_s$  for the Hybrid Reinforced Concrete that provides the use of fibre and steel bars;
- FRC $f_{R3k}$ - $\rho_s$  for the Fibre Reinforced Concrete that provides only steel fibre.

Fibre dosage [ $Kg/m^3$ ]	$f_{R3k}$ [ $Mpa$ ]	Fibre aspect ratio [-]	Fibre tensile strength [ $Gpa$ ]
0	0		
15	2,1		
20	2,7		
25	3,4		
30	4,1	80	2
40	5,5		
50	6,9		
60	8,2		
70	9,6		

**Table 5.3:** Fibre properties [23]

The optimisation are represented in the Table and Figure:

<i>Code</i>	$f_{R3k}$ [Mpa]	Internal spans [ $mm^2/m$ ]		External spans [ $mm^2/m$ ]	
		As,b	As,t	As,b	As,t
ORC-0.86	0	524,7	1197	639,7	1210,3
HRC2.1	2,1	402,2	912,1	522,2	925,6
HRC2.7	2,7	367,4	831,5	492,4	831,5
HRC3.4	3,4	326,7	738,0	451,7	741,6
HRC4.1	4,1	286,2	645,0	411,2	658,2
HRC5.5	5,5	205,2	460,7	335,2	465
HRC6.9	6,9	124,5	278,5	259,5	278,2
HRC8.2	8,2	49,8	111,0	184,8	125
FRC9.6	9,6	0	0	95	17

**Table 5.4:** Amount of top and bottom reinforcement in the optimised hybrid flat slab for  $mm^2/m$  at ULS

The solution ORC-0.86 is without fibres, the solution FRC9.6 has a low almost zero quantity of steel rebars.

<i>Code</i>	Total steel content		
	Fibre [ $kg/m^3$ ]	Rebars	Total
ORC-0.86	0	62.5	62.5
HRC2.1	15	49.1	64.1
HRC2.7	20	45.3	65.3
HRC3.4	25	40.9	65.9
HRC4.1	30	36.4	66.4
HRC5.5	40	27.6	67.6
HRC6.9	50	18.9	68.9
HRC8.2	60	10.8	70.8
FRC9.6	70	3.8	73.8

**Table 5.5:** Total steel content in the optimised hybrid flat slab at ULS  $Kg/m^3$

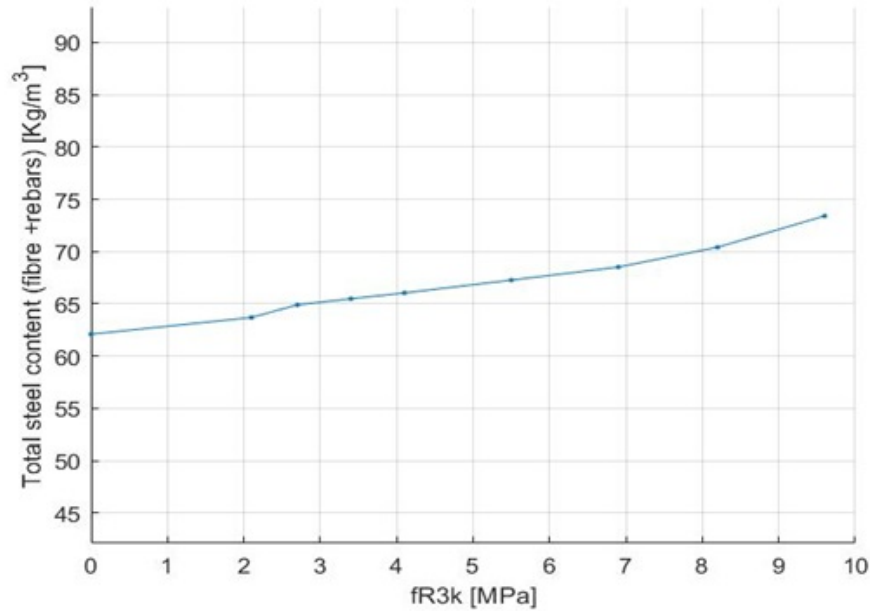


Figure 5.4: Total amount of steel (fibre+rebar) in relation to  $f_{R3k}$

### 5.3 Hybrid Solution for flat slabs at SLS

The previous subchapter presented the options of the hybrid solution for the particular flat slab at ULS (Figure 5.4). These results will serve as a starting point for the study in question which, in turn, is focused on the behaviour of the flat slab under ULS and SLS, particularly, on crack width estimation under different values of load. Since the Yield Line Method does not provide sufficient information regarding the moment distribution over the slab, the elastic analysis was carried out by means of finite element program. Thereafter, effect of the presence of fibres in the concrete mix and, as a consequence, the increased residual tensile strength was studied in relation to different values of loads. It should be highlighted that the determination of crack width has been obtained in quasi-permanent load condition of slab ( $Q_d = G_k + \sum_{j=1}^n \psi_{2j} \cdot Q_{kj}$ )[9], where:

DEAD [ $KN/m^2$ ]		LIVE [ $KN/m^2$ ]
G1 (permanent structural)	G2 (permanent no structural)	Q (according to use)
4.8	2	$4 \cdot \psi_2 (= 0.6)$
<b>9.2 [<math>KN/m^2</math>]</b>		

**Table 5.6:** Quasi-permanent combination load[24]

The map of moments is represented in Figure 5.5 (as the spans are equal in X and Y directions, the moments are also equal in both directions).

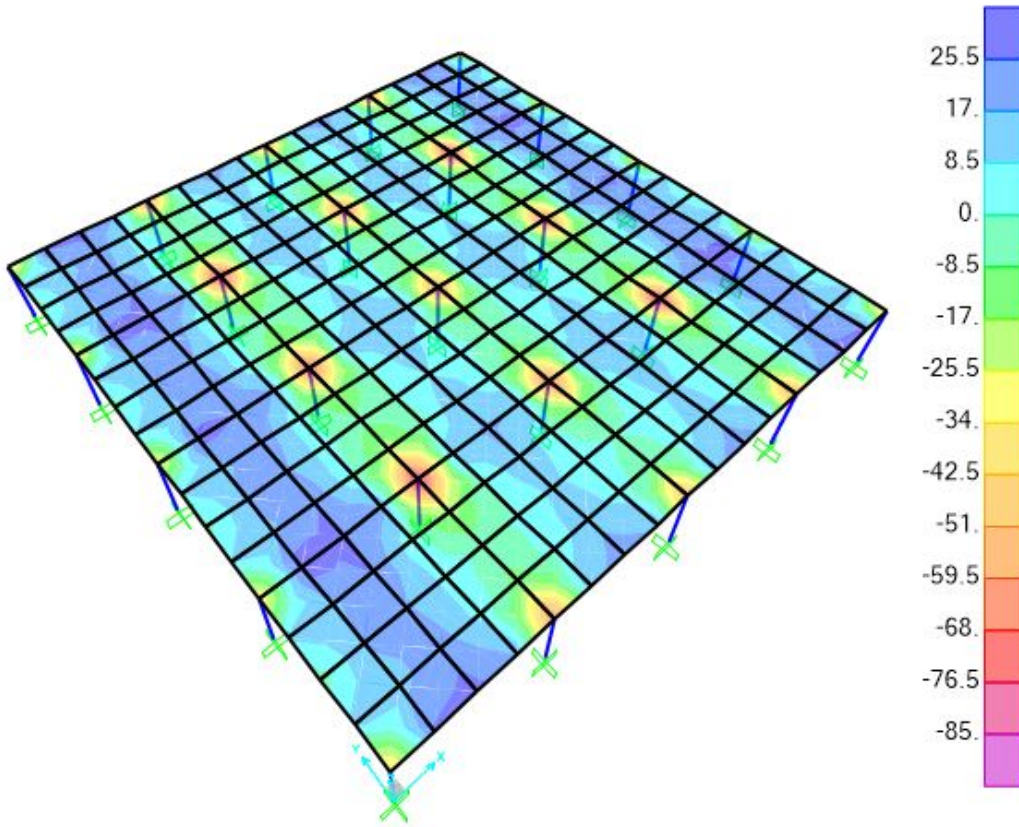


**Figure 5.5:** Elastic moment distribution in quasi-permanent load combination

As it possible to appreciate in the Figure above, the maximum values (positive and negative) of the moments are:  $M_{max}=31.85 KNm$   $M_{min}=-88.85 KNm$

$KNm$ . The  $M_{cr} = 38.23KNm$ . Taking into account there is a linear relationship between applied load and produced moments, that next function could be obtained:

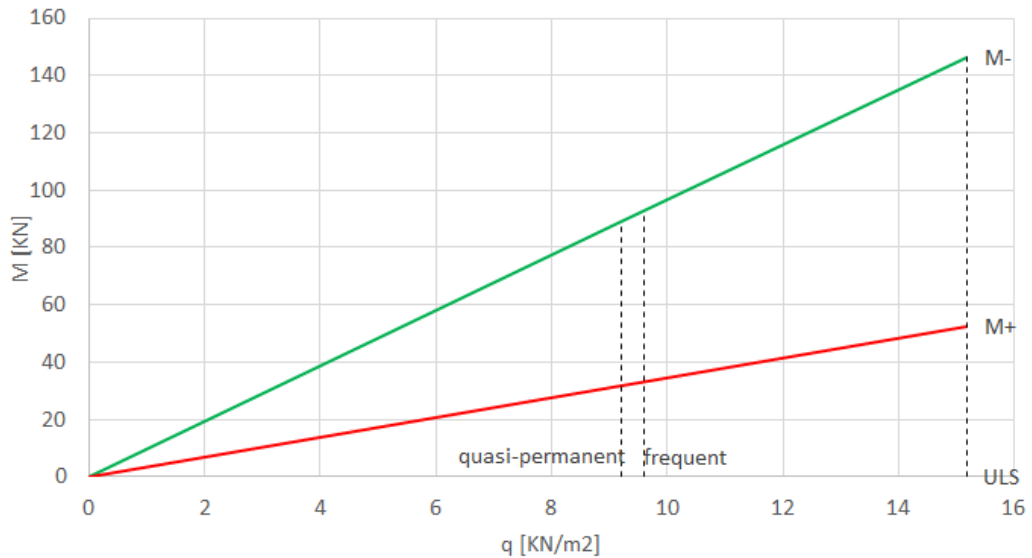


**Figure 5.6:** Load-Moment relationship for the structure in question

### 5.3.1 Calculation plane deformation and crack width

For the calculation of the crack width it needs to obtain the value of the stress-strain steel and thus the plane deformation, given external forces:  $N_{est}$  and  $M_{est}$ . It has been done with Newton Rapshon method (see Annex A). It is an iterative calculation with the aim of balancing the internal forces generated by the tensional plane and resistance of the materials with the external forces.

## 5.4 Results

The analysis has been carried out varying the value of uniformly distributed load ( $kN/m^2$ ) and evaluating the effect of the load increment on the crack width for different hybrid solutions. These crack width were calculated in accordance with the Equation 3.10 (see Chapter 3.4)

q [KN/m]	Q/Q <sub>cr</sub>	M-[KNm]	q [KN]	Q/Q <sub>cr</sub>	M+[KNm]
3.96	1.00	<b>38.23</b>	4.80	1.00	16.62
4.53	1.14	43.66	6.80	1.42	23.54
4.80	1.21	46.30	9.20	1.92	<b>31.85</b>
5.42	1.37	52.25	10.98	2.29	38.00
5.70	1.44	55.00	11.04	2.30	38.23
6.39	1.61	61.64	11.45	2.38	39.63
6.80	1.72	65.60	11.75	2.45	40.68
7.38	1.86	71.18	12.28	2.56	42.50
7.59	1.91	73.20			
7.88	1.99	76.01			
8.37	2.11	80.71			
8.76	2.21	84.45			
9.21	2.32	<b>88.80</b>			

**Table 5.7:** Applied load/produced external moment

The model used is the rigid-plastic. Since the study was conducted at the SLS, the tensile strength concrete taken into account is  $f_{Fts}$ , derived from Equation 2.10. The study was conducted for different values of  $f_{R3k}$  listed in the Table 5.4 and for different classes of fiber: *b*, *c*, *d*. Following the classification of SFRC described in Chapter 2.4.6 [14], the value of  $f_{R1k}$  was obtained by applying of a ratio factor ( $f_{R3k}/f_{R1k}$  =ratio factor) respectively equal to:

- 0.75 for class *b*;
- 1 for class *c*;
- 1.3 for class *d*.

Also, it should be mentioned that the characteristic values have been converted into mean values  $f_{R1m}$ ,  $f_{R3m}$ ,  $f_{Ftsm}$  (Equation 2.16), in accordance with the provided equations for the calculations of crack widths [9].

### Influence of amount of fibre $Kg/m^3$ or flexural residual strength $f_{R3k}$

The first results obtained were in order to study the contribution of the amount of fiber ( $Kg/m^3$ )/ $f_{R3k}$ , according to Minelli [23], in the crack opening. In the Figure 5.7 these values have been reported considering different percentage of reinforcement  $\rho_s$ .

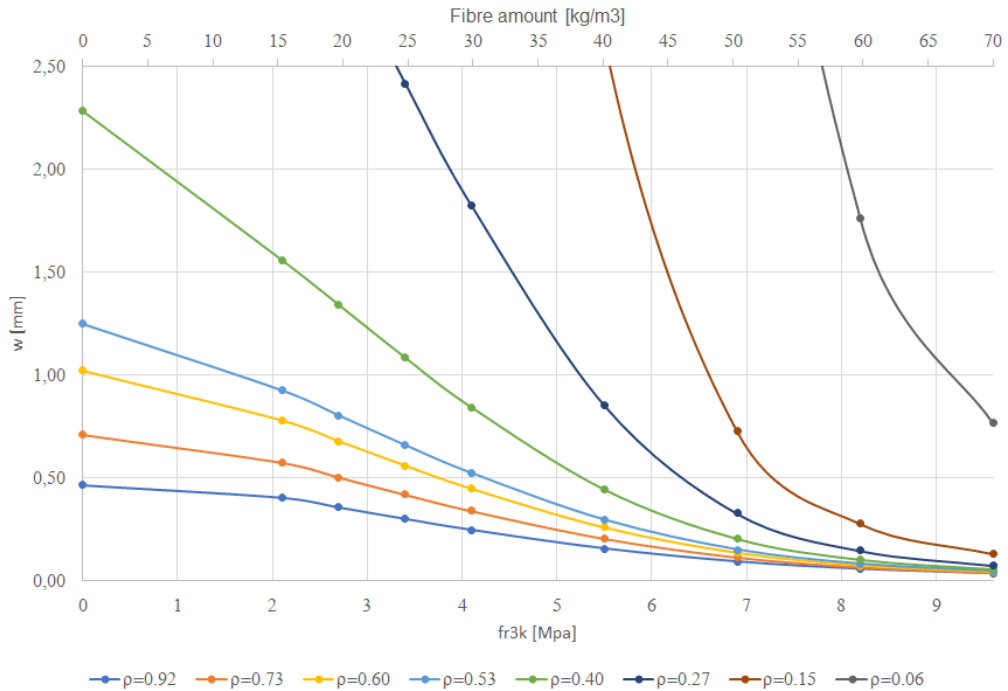


**Figure 5.7:** Amount of fibre - Crack width for different  $\rho_s$ . External panel.  $M_{qp} = 88.8KNm$ . Ratio 0.75

The load applied is quasi-permanent combination load, which in case study generates on the external panel a negative moment of  $88.8 KNm$ . The same verification has not been carried out for the positive moment since it is less than the cracking one ( $M_{qp} \leq M_{cr}$ ). The trend of the curves confirms the clear contribution of the fiber to the crack closing. In the particular case of no-reinforcement ( $\rho_s = 0$ ), it can be noted that the values of  $w_k$  are reduced, albeit insufficiently, from  $w_k = \infty$  (plane concrete) to orders of magnitude lower. In addition, the curves tend to stabilise at the end, highlighting a greater contribution of the reinforcement in the closing crack. In

conclusion, by increasing the amount of fiber and fixing the same amount of reinforcement, it can be deduced from the Figure 5.7, that it helps the ordinary reinforcement in the closing of the crack, unloading the bars tensionally, however the most important contribution is given by the reinforcement.

### Influence of the residual strength ratio ( $f_{R3k}/f_{R1k}$ )

The previous calculation was repeated for different fibre classes, in particular  $b$  ( $=0.75$ ),  $c$  ( $=1$ ),  $d$  ( $=1.3$ ). Below an example of the behavior of each class, fixed  $\rho_s=0.4$ .

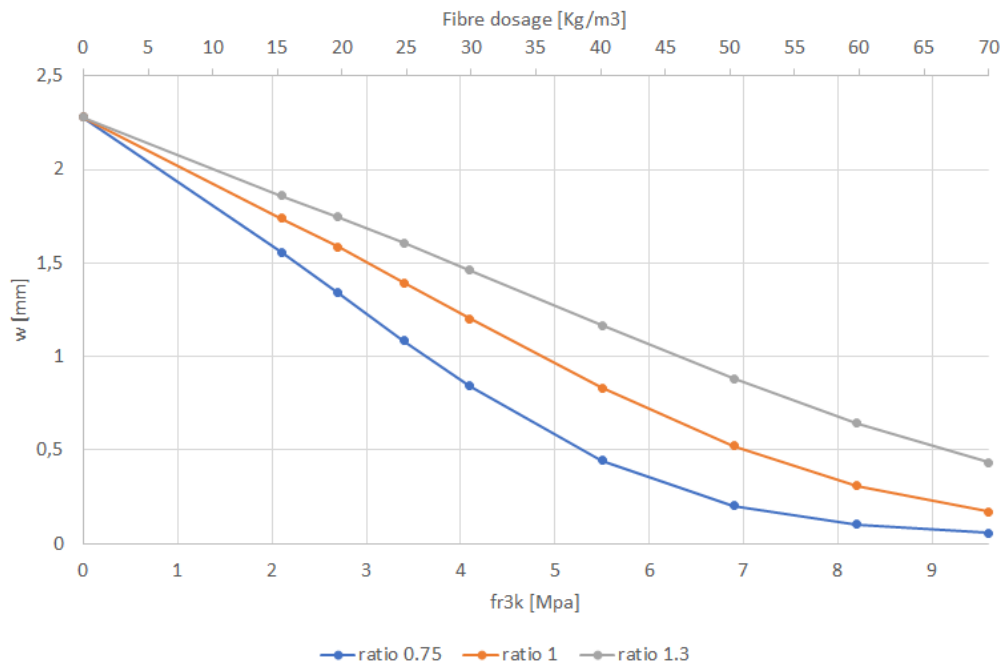


**Figure 5.8:** Amount of fibre - Crack width for  $\rho_s=0.4$  and different class fibre. External panel.  $M_{qp} = 88.8KNm$

In all the simulations, it was observed that the fiber class  $b$ , with ratio 0.75, has a better behaviour in the control crack than the other classes that instead having better behaviour at ULS. The Figure 5.9 demonstrate the same effect of increasing of  $f_{Fts}$  on the crack width. It should be added the the increment of load ( $x$  axis) is normalised to the one which provokes the first cracks,  $Q/Q_{cr} = 2.32$  corresponds to the quasi-permanent load combination.

The following graph represents a hybrid solution, in which the values of  $\rho_s$  and  $f_{R3k}$  are fixed.

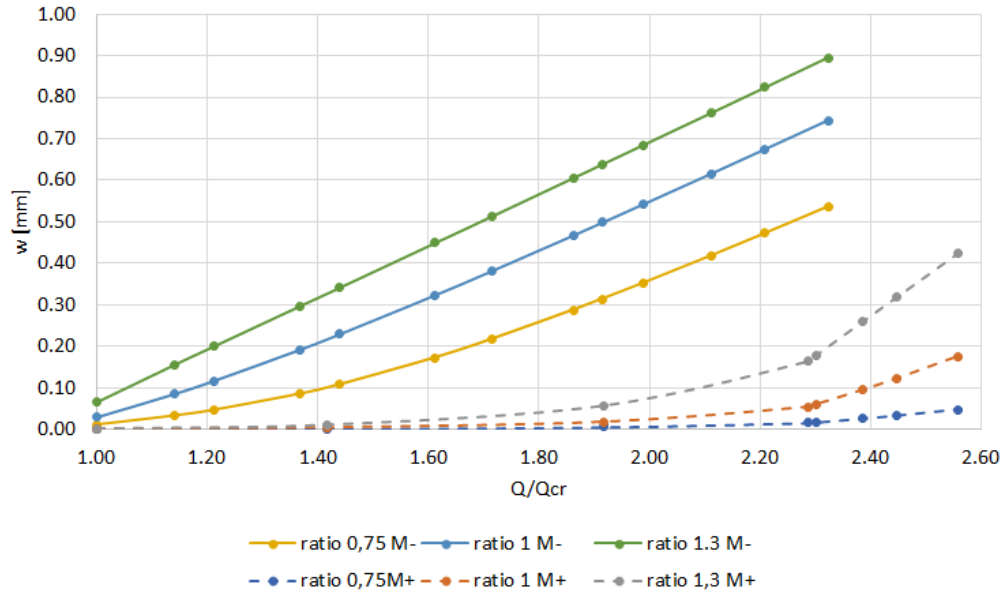


**Figure 5.9:** Applied Load - Crack Width relationship for established Hybrid Solution HRC4.1-0.4 (int)

### Crack width in internal panel and external panel at $M^+$ and $M^-$

In all cases, the design of the external panels is more critical than the internal ones, since the lateral support of the edge is missing, the crack openings will be larger with smaller loads. This concept is evident in the Figure 5.10 where it can also be seen that: for M- the high crack opening values are reached more exponentially than for M+. The reinforcement solutions presented are those that meet the requirements of the ULS.

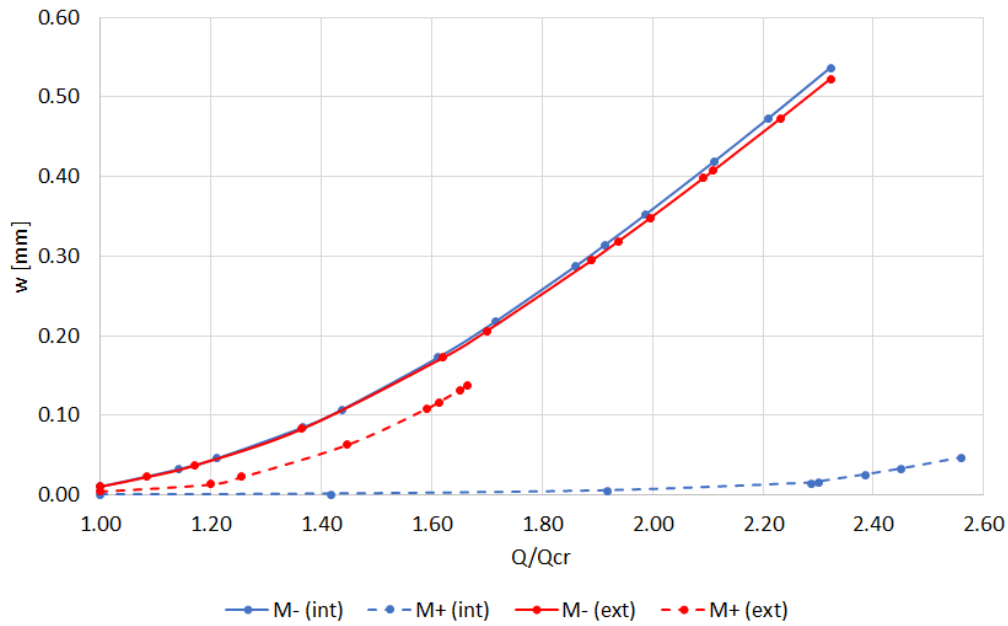


**Figure 5.10:** Comparison of crack width for positive and negative moment, internal and external panel, reinforcement HRC4.1

### Different Hybrid Solutions - Crack Widths

The presence of fibres is of paramount importance in terms of crack control as it was discussed previously. However the hybrid solutions has not been studied in detail yet. In this paragraph was made a study changing both parameters:  $f_{R3k}$  and  $\rho_s$ . Therefore, based on Sutera's calculations at ULS (see Table 5.4), several options were chosen and the areas with maximum negative moments (above columns) were evaluated in terms of crack widths under different load magnitudes. The results of some particular reinforcement solutions for the external panel could be appreciated below in Figure 5.11 and Table 5.8.

$\backslash Code$	ORC	HRC	HRC	HRC	FRC
$f_{R3k}$	0	2.7	4.1	8.2	9.6
$\rho_s$	0.92	0.66	0.53	0.15	0.06
$A_{s,b} [mm^2/m]$	639.70	492.40	411.20	184.80	95.00
$A_{s,t} [mm^2/m]$	1210.30	831.50	658.20	125.00	17.00
Q/Q <sub>cr</sub>	w [mm]				
1.00	0,13	0,04	0,01	0,00	0,00
1.09	0,16	0,07	0,02	0,00	0,01
1.17	0,20	0,10	0,04	0,01	0,02
1.37	0,26	0,18	0,08	0,02	0,04
1.62	0,35	0,28	0,17	0,04	0,11
1.70	0,37	0,32	0,21	0,05	0,14
1.89	0,43	0,39	0,29	0,09	0,24
1.94	0,44	0,42	0,32	0,10	0,28
2.00	0,46	0,44	0,35	0,12	0,33
2.09	0,49	0,48	0,40	0,15	0,42
2.11	0,49	0,49	0,41	0,16	0,45
2.23	0,53	0,54	0,47	0,22	0,61
2.32	0,56	0,58	0,52	0,28	0,77

**Table 5.8:** Applied Load - Crack Widths for different reinforcement solutions

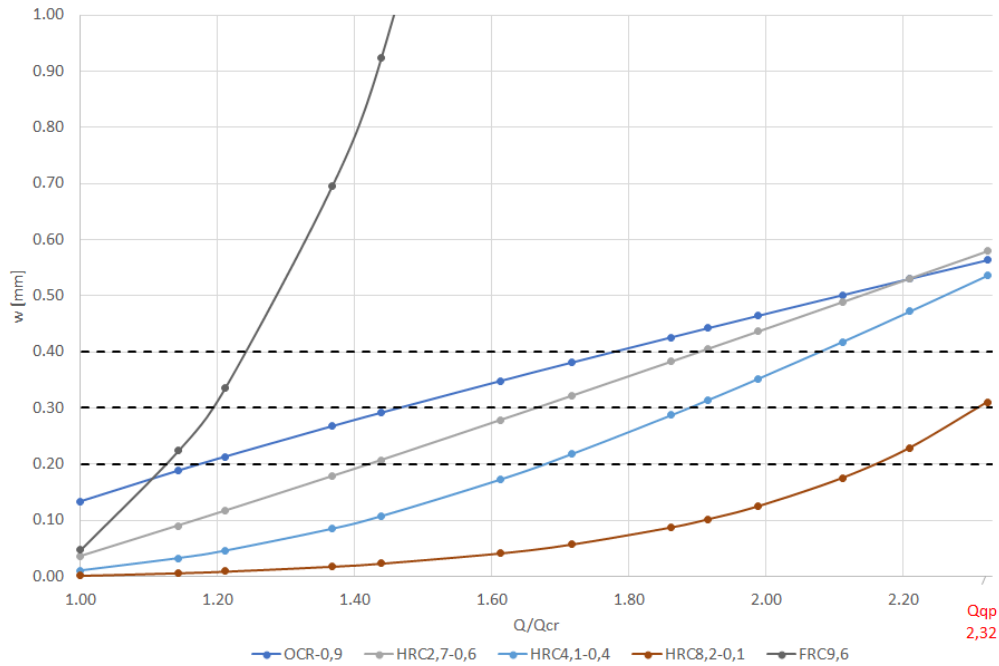


**Figure 5.11:** Applied Load - Crack Widths for different Hybrid Solutions

The behaviour of reinforcement solutions that have a high  $f_{R3k}$  present better performance than the traditional solution (ORC-0.9), even when  $\rho_s$  is low. However, the solution that provides for the total absence of reinforcement (FRC9.6) does not respond perform well, as it takes a strongly exponential trend in the function of crack opening and load.

## 5.5 Crack Width Limits at SLS

For the quasi-permanent load combination at SLS the certain values of crack width are allowed in dependence in the exposure class as it possible appreciate below:

Exposure Class	Reinforced members and prestressed members with unbonded tendons	Prestressed members with bonded tendons
	Quasi-permanent load combination	Frequent load combination
X0, XC1	0,4 <sup>1</sup>	0,3
XC2, XC3, XC4	0,3	0,2 <sup>2</sup>
XD1, XD2, XD3, XS1, XS2, XS3		Decompression
<p><b>Note 1:</b> For X0, XC1 exposure classes, crack width has no influence on durability and this limit is set to give generally acceptable appearance. In the absence of appearance conditions this limit may be relaxed.</p> <p><b>Note 2:</b> For these exposure classes, in addition, decompression should be checked under the quasi-permanent combination of loads.</p>		

**Figure 5.12:** Recommended values of  $w_{max}$  (mm) [15]

Exposure class	Steel fibre reinforced concrete without additional steel rebar reinforcement
X0, XC1	0.4
XC2, XC3	0.3
XC4, XD1, XS1	0.2

**Table 5.9:** Recommendation for SFRC  $w_{max}$  [mm]

For X0, XC1 exposure classes, crack width has no influence on durability and this limit is set to guarantee acceptable appearance. In the absence of appearance conditions this limit may be relaxed.

## 5.6 Comparison of achieved results with permitted crack widths

The verifications consisted in checking in quasi-permanent load combination ( $M_{max}^- = 88.8KNm$  and a  $M_{max}^+ = 31.85KNm$ ) if the reinforcement designed at the ULS (Table 5.4) is enough to meet the requirements for cracks opening at 0.2, 0.3, 0.4 mm. If that doesn't work, the required amount of reinforcement has been calculated. In the Table 5.10 Table 5.10 has been shown the values of crack width in quasi-permanent combination load for the internal and external panel and considering all aspect ratio. Since the ULS designed

reinforcement meets the requirements at SLS for positive moment, because  $M_{qp}^+ < M_{cr}$  only the negative moment will be analysed.

	INTERNAL			EXTERNAL			
	0.75	1	1.3	0.75	1	1.3	
OCR-0.86	0.56	0.56	0.56	OCR-0.92	0.56	0.56	0.56
HRC2.1-0.66	0.58	0.65	0.69	HRC2.1-0.72	0.57	0.63	0.67
HRC2.7-60	0.58	0.67	0.74	HRC2.7-66	0.58	0.67	0.74
HRC3.4-0.53	0.56	0.71	0.81	HRC3.4-0.59	0.56	0.70	0.80
HRC4.1-0.47	0.54	0.74	0.90	HRC4.1-0.53	0.52	0.72	0.87
HRC5.5-0.33	0.45	0.84	1.18	HRC5.5-0.4	0.44	0.83	1.17
HRC6.9-0.2	0.33	1.04	1.91	HRC6.9-0.26	0.33	1.04	1.92
HRC8.2-0.08	0.31	1.67	5.75	HRC8.2-0.15	0.28	1.44	4.73
FRC9.6	12.63	69.59	2014.19	FRC9.6-0.05	0.77	4.08	48.30

**Table 5.10:** Crack width in internal and external panel at  $M_{qp}^-$  for different ratio. Maximum crack width= 0.4mm

	INTERNAL			EXTERNAL			
	0.75	1	1.3	0.75	1	1.3	
OCR-0.86	0.56	0.56	0.56	OCR-0.92	0.56	0.56	0.56
HRC2.1-0.66	0.58	0.65	0.69	HRC2.1-0.72	0.57	0.63	0.67
HRC2.7-60	0.58	0.67	0.74	HRC2.7-66	0.58	0.67	0.74
HRC3.4-0.53	0.56	0.71	0.81	HRC3.4-0.59	0.56	0.70	0.80
HRC4.1-0.47	0.54	0.74	0.90	HRC4.1-0.53	0.52	0.72	0.87
HRC5.5-0.33	0.45	0.84	1.18	HRC5.5-0.4	0.44	0.83	1.17
HRC6.9-0.2	0.33	1.04	1.91	HRC6.9-0.26	0.33	1.04	1.92
HRC8.2-0.08	0.31	1.67	5.75	HRC8.2-0.15	0.28	1.44	4.73
FRC9.6	12.63	69.59	2014.19	FRC9.6-0.05	0.77	4.08	48.30

**Table 5.11:** Crack width in internal and external panel at  $M_{qp}^-$  for different ratio. Maximum crack width= 0.3mm

It's clear that the class *b* fibre meets the requirements at quasi-permanent load combination better than the class *c* and *d*, but the designed reinforcement is not always sufficient to ensure SLS. The fibre improves the response at SLS, in particular the increase of  $f_{R3k}$ , as already shown, is the most important parameter. However, extreme conditions which provide for the almost amount of steel bars reinforcement in favour of a high  $f_{R3k}$  do not respond positively to the requirements of maximum crack opening. To better understand the trend, the results of the Table 5.11 5.10 have been graphed in the Figure 5.14.

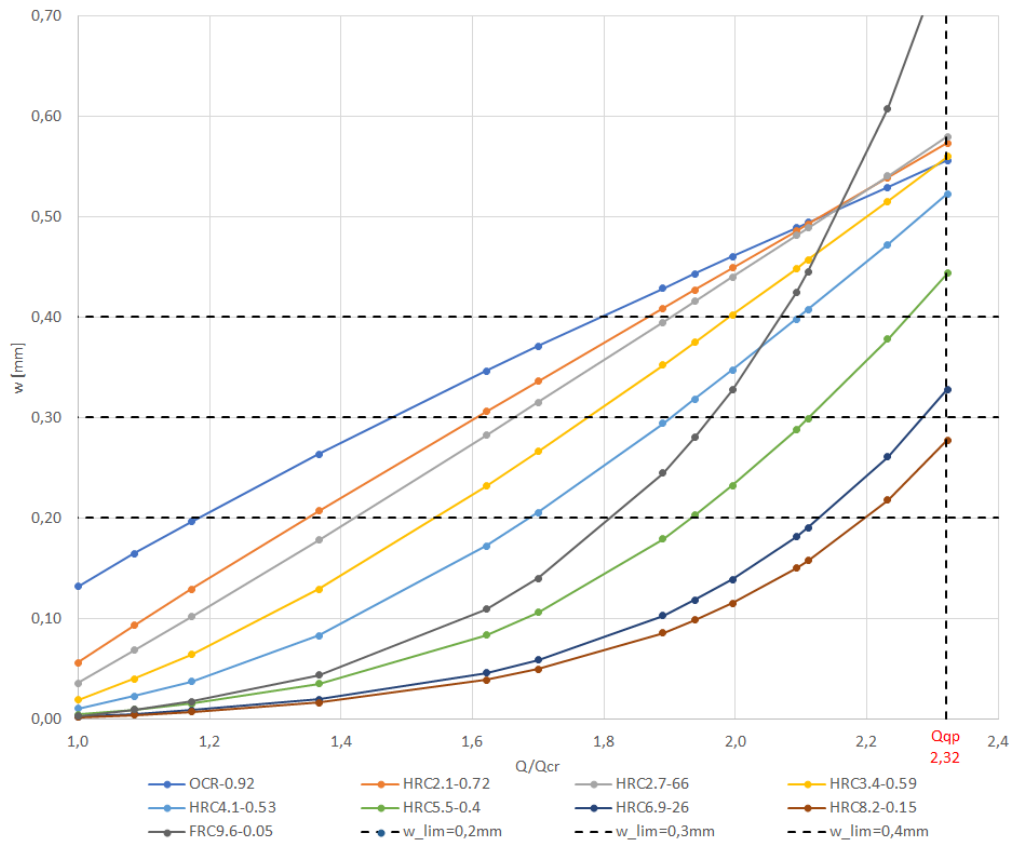


**Figure 5.13:** Applied Load - Crack Widths verification for different Hybrid Solutions. External panel

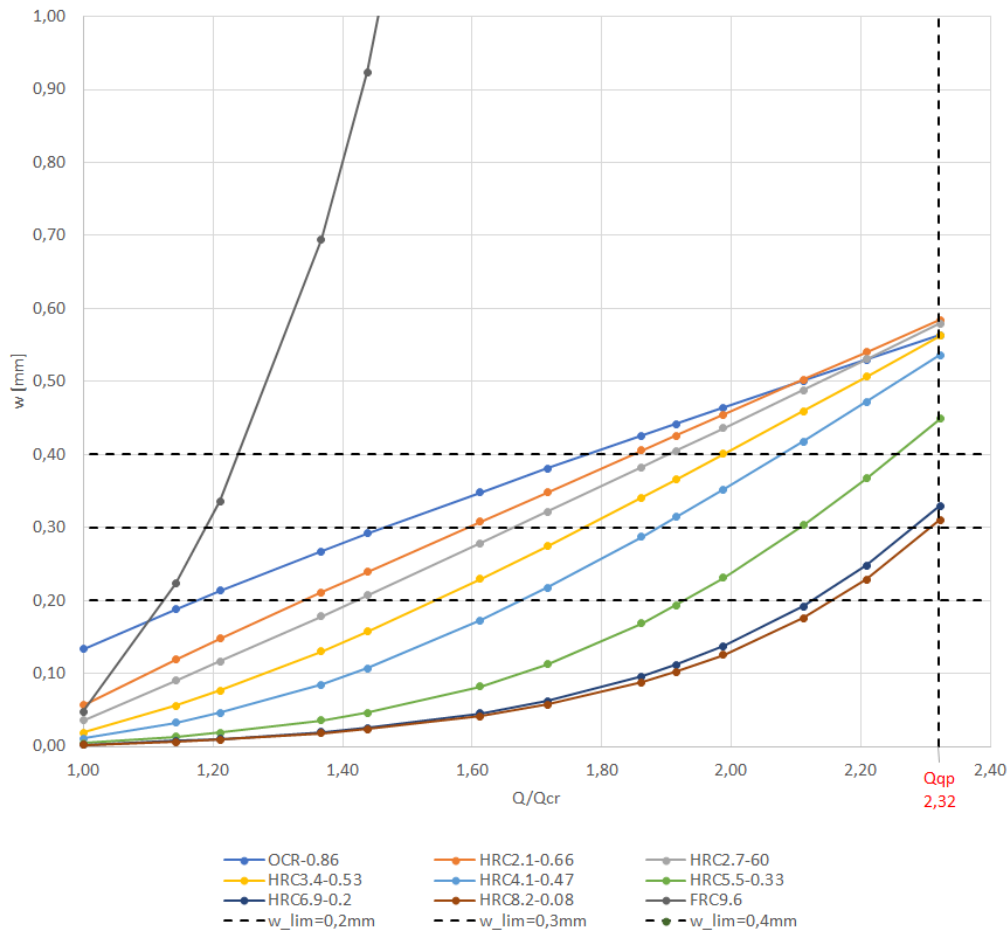


**Figure 5.14:** Applied Load - Crack Widths verification for different Hybrid Solutions. Internal panel

## 5.7 Design of additional steel reinforcement at SLS

For Hybrid Solutions which did not meet the SLS requirements, the additional reinforcement was implemented. As it was highlighted previously, the areas near the columns (with maximum negative moment) were the ones where the designed at ULS reinforcement was insufficient. Table 5.14 5.13 5.12 presents the required amount of the additional reinforcement for permitted crack widths (0.4, 0.3 and 0.2 mm).

	INTERNAL PANEL				EXTERNAL PANEL			
	$A_{sb,ULS}$	$A_{sb,SLS}$	$A_{sb,add}$	$\Delta A_s/A_s$	$A_{sb,ULS}$	$A_{sb,SLS}$	$A_{sb,add}$	$\Delta A_s/A_s$
	$mm^2/m$				$mm^2/m$			
OCR	1197.56	2162.6	965.0	0.8	1210.30	2165.3	955.0	0.8
HRC2.1	912.14	2172.1	1260.0	1.4	925.60	2175.6	1250.0	1.4
HRC2.7	831.54	1971.5	1140.0	1.4	831.50	1971.5	1140.0	1.4
HRC3.4	738.03	1723.0	985.0	1.3	741.60	1721.6	980.0	1.3
HRC4.1	645.07	1470.1	825.0	1.3	658.20	1468.2	810.0	1.2
HRC5.5	460.74	955.7	495.0	1.1	465.00	955	490.0	1.1
HRC6.9	278.48	483.5	205.0	0.7	278.20	478.2	200.0	0.7
HRC8.2	111.03	191.0	80.0	0.7	125.00	190	65.0	0.5
FRC9.6	0.00	80.0	80.0	8	17.00	77	60.0	3.5

**Table 5.12:** The required amount of additional reinforcement at SLS ( $w_{max}=0.2mm$ ,  $f_{R3k}/f_{R1k}=0.75$ )

	INTERNAL PANEL				EXTERNAL PANEL			
	$A_{sb,ULS}$	$A_{sb,SLS}$	$A_{sb,add}$	$\Delta A_s/A_s$	$A_{sb,ULS}$	$A_{sb,SLS}$	$A_{sb,add}$	$\Delta A_s/A_s$
	$mm^2/m$				$mm^2/m$			
OCR	1197.56	1627.6	430.0	0.2	1210.30	1625.30	415.0	0.1
HRC2.1	912.14	1647.1	735.0	0.3	925.60	1535.60	610.0	0.2
HRC2.7	831.54	1516.5	685.0	0.3	831.50	1391.50	560.0	0.2
HRC3.4	738.03	1343.0	605.0	0.4	741.60	1211.6	470.0	0.2
HRC4.1	645.07	1140.1	495.0	0.3	658.20	1028.2	370.0	0.2
HRC5.5	460.74	670.7	210.0	0.2	465.00	655	190.0	0.1
HRC6.9	278.48	308.5	30.0	0.1	278.20	308.2	30.0	0.0
HRC8.2	111.03	116.0	5.0	0.0	125.00	125	0.0	0.0
FRC9.6	0.00	50.0	50.0	0.6	17.00	47	30.0	0.4

**Table 5.13:** The required amount of additional reinforcement at SLS ( $w_{max}=0.3mm$ ,  $f_{R3k}/f_{R1k}=0.75$ )

	INTERNAL PANEL				EXTERNAL PANEL			
	$A_{sb,ULS}$	$A_{sb,SLS}$	$A_{sb,add}$	$\Delta A_s/A_s$	$A_{sb,ULS}$	$A_{sb,SLS}$	$A_{sb,add}$	$\Delta A_s/A_s$
	$mm^2/m$				$mm^2/m$			
OCR	1197.56	1342.6	145.0	0.1	1210.30	1340.3	130.0	0.1
HRC2.1	912.14	1647.1	735.0	0.4	925.60	1220.6	295.0	0.2
HRC2.7	831.54	1516.5	685.0	0.5	831.50	1106.5	275.0	0.2
HRC3.4	738.03	1343.0	605.0	0.5	741.60	961.6	220.0	0.2
HRC4.1	645.07	1140.1	495.0	0.4	658.20	813.2	155.0	0.2
HRC5.5	460.74	670.7	210.0	0.3	465.00	510	45.0	0.1
HRC6.9	278.48	278.5	0.0	0.0	278.20	278.2	0.0	0.0
HRC8.2	111.03	111.0	0.0	0.0	125.00	125	0.0	0.0
FRC9.6	0.00	35.0	35.0	0.7	17.00	37	20.0	0.4

**Table 5.14:** The required amount of additional reinforcement at SLS ( $w_{max}=0.4mm$ ,  $f_{R3k}/f_{R1k}=0.75$ )

By placing stricter maximum crack width, the required amount of reinforcement results in those shown in the Figure 5.15.

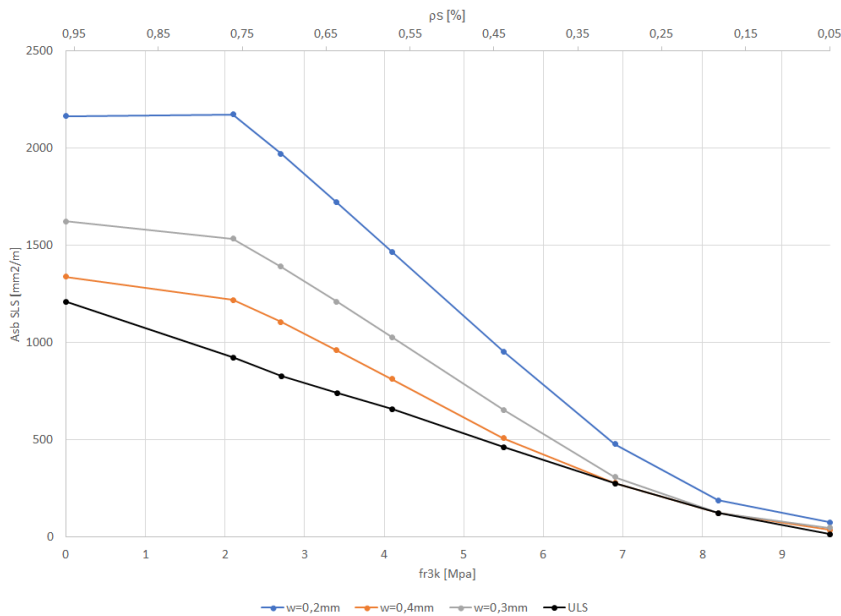


**Figure 5.15:** Designed amount of traditional reinforcement at SLS ( $f_{R3k}/f_{R1k}=0.75$ ). External panel

The case illustrated shows the significant trend of the reinforcement quantity curve required to meet the maximum crack opening 0.2, 0.3, 0.4 mm. The Figure 5.15 shows the amount of reinforcement for an external panel but the trend of the internal one and similar. The quantity of reinforcement necessary to fulfil the requirements tends to decrease with the increase of  $f_{R3k}$ . The reinforcement solutions studied have an indirectly proportional ratio between  $f_{R3k}$  and  $\rho_s$ . The amount of reinforcement required decreases with the increase of  $f_{R3k}$ . However, the first cases, where  $f_{R3k}$  is in a range between 2.1 4.1 Mpa, are more disadvantageous than the traditional solution. In fact, they provide for a slight increase in reinforcement. Obviously, under the most restrictive conditions, the amount of reinforcement required increases. There are cases where the amount of reinforcement designed for the ULS is sufficient or requires a minor addition in order to meet the requirements of the SLS. This case occurs for the same amount of fibres, both in the external and internal panel, and in particular:

- Internal panel: solution HRC6.9-0.20 and HRC8.2-0.08;
- External panel: solution HRC6.9-0.26 and HRC8.2-0.15.

One last consideration can be made in the case of FRC. In the following graph you can see that the fiberless solution, although it meets the requirements of the ULS well, is critical for the SLS. In order to comply with the latter, it is necessary to insert a minimum reinforcement. This is shown in Figure 5.16 in a standardised manner respect to the quantity of reinforcement expected for the ULS. This is justifiable on the basis of the concept explained in the Figure 5.7 where it has been shown that the higher contribute at the closure of the crack is given by the bars reinforcement and the fiber helps to release the stresses in the steel, however it is insufficient to fully meet the requirements.

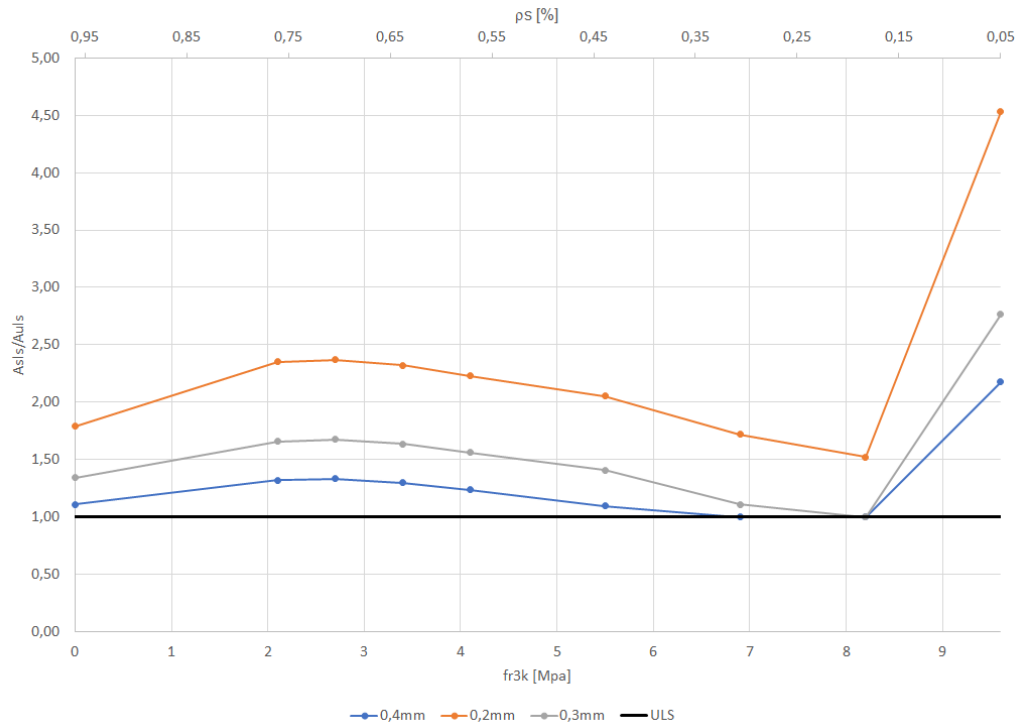


**Figure 5.16:** Ratio ( $A_{s,SLS}/A_{s,ULS}$ ) of quantity of steel bars reinforcement added. Ratio 0.75.

This is reflected for each fibre class and for each requirement.

## 5.8 Total steel content at SLS

It has been calculated the effective quantity of reinforcement in order to meet the requirements studied; for the calculation of  $kg/m^3$  of rebars it has been taken into account the flat slab dimensions, the number of external and internal panels and the design hypotheses described above, in particular the layout scheme of the top and bottom reinforcement (see Figure 5.3), while the fibre dosage ( $kg/m^3$ ) it has been followed the Table 5.3. In the Table 5.15 are showed the total steel content including fibre dosage. The specific steel weight considered is  $7850 kg/m^3$ .

$w_{max}$	ratio	ORC	HRC2.1	HRC2.7	HRC3.4	HRC4.1	HRC5.5	HRC6.9	HRC8.2	FRC9.6
0.4	0.75	75.97	81.69	81.31	79.63	77.91	74.57	71.79	71.87	74.82
	1	75.97	84.00	84.51	83.83	83.09	81.63	80.08	79.35	79.29
	1.3	75.97	85.54	86.56	86.56	86.56	86.46	86.23	86.48	86.89
0.3	0.75	68.44	73.28	73.79	73.11	72.27	70.45	69.39	70.92	74.40
	1	68.44	74.89	76.05	76.19	76.19	76.06	75.70	76.00	77.24
	1.3	68.44	75.93	77.45	78.10	78.63	79.72	80.57	81.75	82.88
0.2	0.75	75.97	81.69	81.31	79.63	77.91	74.57	71.79	71.87	74.82
	1	75.97	84.00	84.51	83.83	83.09	81.63	80.08	79.35	79.29
	1.3	75.97	85.54	86.56	86.56	86.56	86.46	86.23	86.48	86.89

**Table 5.15:** Total steel content: fibre + rebars  $kg/m^3$

In order to better understand the behaviour of each solution, the data in the Table 5.15 have been shown in relation to the displayed depending on the maximum crack width set or the fiber class.

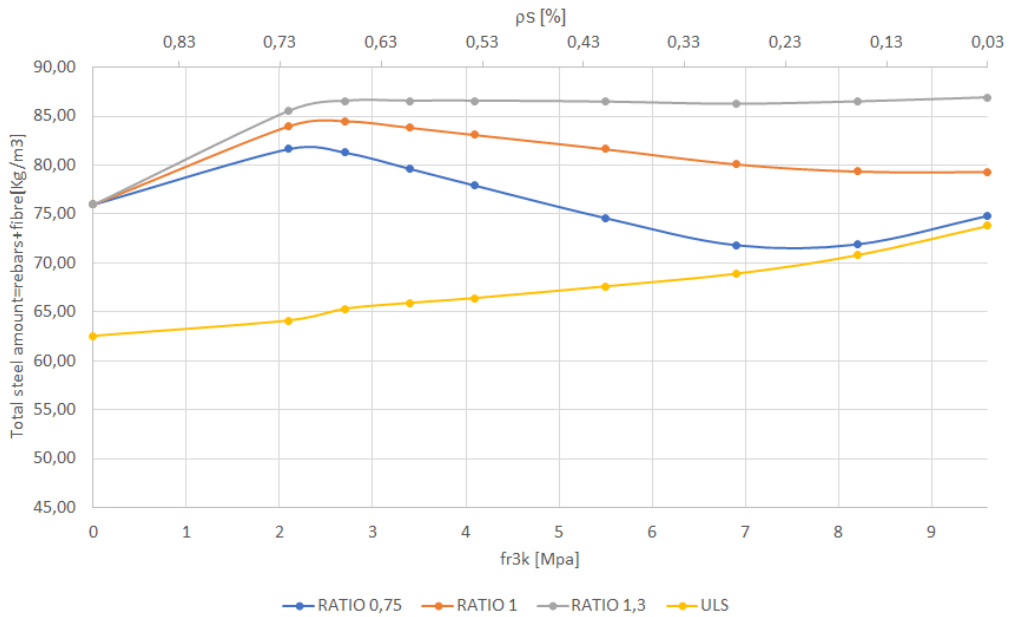


**Figure 5.17:** Total steel content. Maximum crack width 0.2 mm

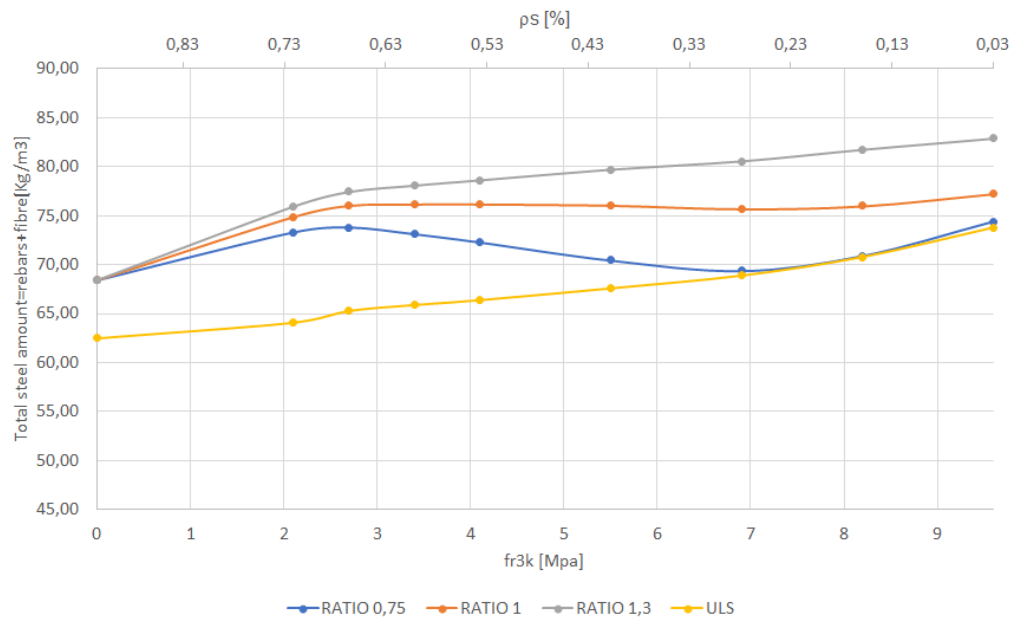


Figure 5.18: Total steel content. Maximum crack width 0.3 mm

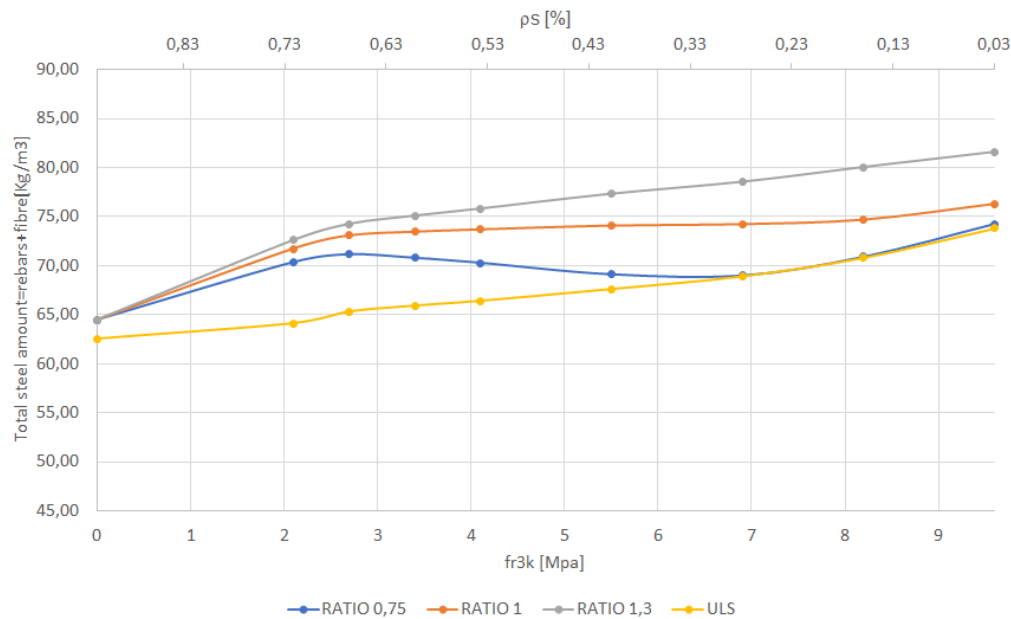


Figure 5.19: Total steel content. Maximum crack width 0.4 mm

In the figures the quantity of steel used in relation to the  $f_{R3k}$  and  $\rho_s$

has been calculated for the three requirements studied. Each curve considers a different class of steel. The class *b* fibers allow to meet the requirements and at SLS and in the same time use fewer amounts of steel for higher  $f_{R3k}$  and  $\rho_s$ . The previous graphs show a downward trend, this means that the fiber plays an important role in closing crack. The quantities designed at the ULS need less additions for the SLS. The other two classes *c* and *d* have bad performance, in the graphs the trend is more stable or increasing. This means that those quantities of fiber and reinforcement designed for ULS are not enough to SLS for solutions where  $\rho_s$  decreases, in fact they require additions of reinforcement gradually greater than ULS. Going into more detail on the behaviour of class *b* fibre and comparing the required steel quantities with those at the ULS, in the Figure 5.20, a range of  $f_{R3k}$  is evident where the quantity of fiber contributes more in the control of the crack. The descending branch in question is included in the values  $20Kg/m^3$  and  $50Kg/m^3$  fibre content (corresponding to  $f_{R3k} = 2.7 - 6.9$  Mpa) and respectively  $\rho_s = 0.6 - 0.26$ , after a minimum point ( $f_{R3k} = 6.9$  Mpa,  $50Kg/m^3$  fibre dosage,  $\rho_s = 0.26$ ) the trend of the curve assumes a growing behaviour because it must be remembered that were considered hybrid solutions in which the increase of  $f_{R3k}$  the quantity of traditional reinforcement is gradually less. As already demonstrated, the tail of the curve is representative of solutions in which the reinforcement tends to zero and for this reason the fiber is not able to meet the requirements. Obviously, more restrictive requirements imply higher reinforcement additions. Another important consideration is that the traditional reinforcement solution for smallest values of  $w_{max}$  tends to be gradually more disadvantageous in terms of the amount of steel used.

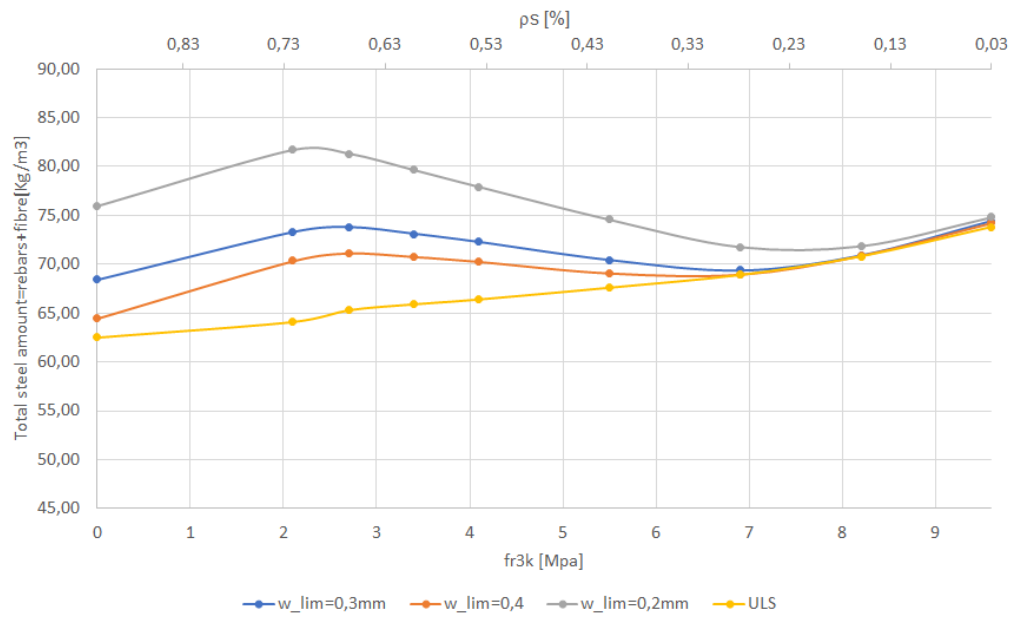


Figure 5.20: Optimization points:  $f_{R3k}-\rho_s$

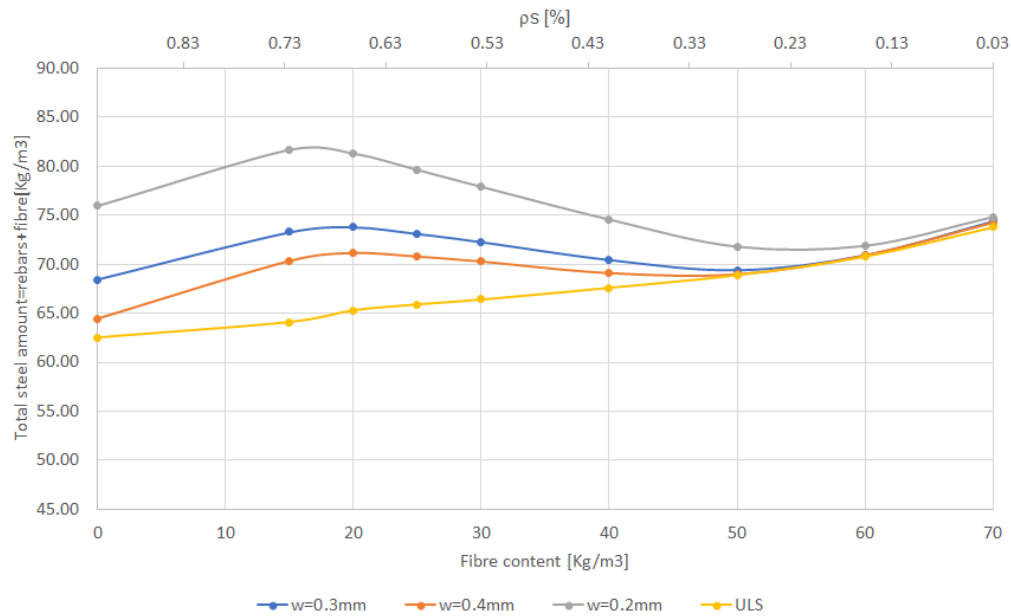


Figure 5.21: Optimization points:  $f_{R3k}-kg/m^3$

## 5.9 Stress limitations

It should be mentioned that the SLS requires during the design not only the limit state of opening cracking in order to satisfy requirements concerning functionality, durability or appearance, but also a certain stress limitations. In fact, the high compressive stresses in the concrete can cause longitudinal microcracks with consequent problems of durability or excessive viscous deformations; tensile stresses in the steel under serviceability conditions should be reduced in order not to provoke the inelastic deformations in the structure. The stress in the structure should be limited to the next values (according to EHE08 [9] and NTC18 [24]):

$$\begin{aligned}\sigma_c &\leq 0.45f_{ck} \\ \sigma_s &\leq 0.8f_{yk}\end{aligned}\tag{5.1}$$

In the following graphs Figure 5.22 5.23 5.24 a comparison is made between the curves previously obtained (Figure 5.20) and the curves that indicate the optimal amount of steel for each effective reinforcement ratio ( $= A_s/A_c$ ) ( $\rho_s$ ) and  $f_{R3k}$ , including not only the requirements for opening crack, but also those of tension limitations mentioned above.

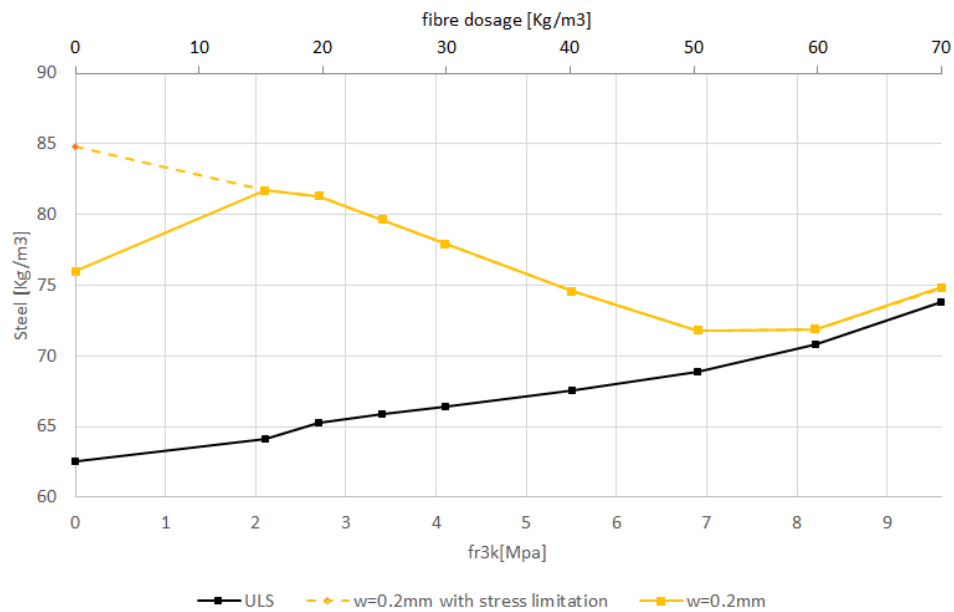


**Figure 5.22:** Total steel content. Maximum crack width= 0.2mm and stress limitation

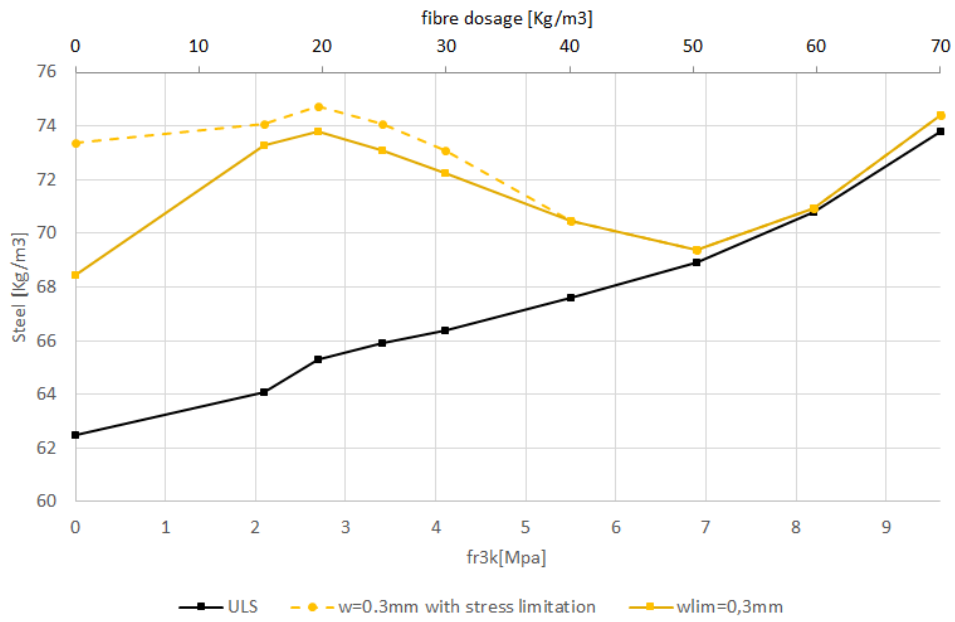


**Figure 5.23:** Total steel content. Maximum crack width= 0.3mm and stress limitation

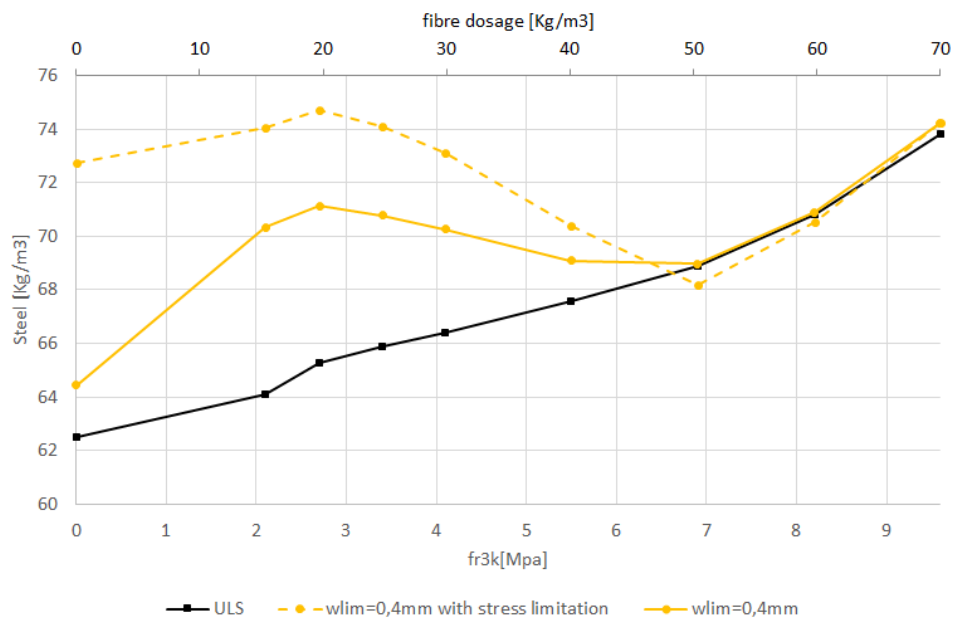


**Figure 5.24:** Total steel content. Maximum crack width= 0.4mm and stress limitation

Additional constraints include further increases in the calculation of traditional reinforcement quantities, particularly where I have low fibre dosage. In less restrictive cases, the reinforcement required to meet the tension requirements also extends to larger fibre dosages, until  $50\text{Kg}/\text{m}^3$ . In the case of  $w_{max}=0.2\text{mm}$  the designed reinforcement is capable of meeting the tension requirements and crack controls. In particular, the further addition is required only in the case of ORC where the contribution of the fiber in reducing the stresses in the steel is lacking.

## 5.10 Economic aspect

The results obtained have been analysed from an economic point of view. The calculation was made in a general way, taking into account only the cost of the material and its installation. These values can give a general idea for a possible future development with regard to the sustainability, in particular economic, of this new solution. The costs and their deviation considered are:

- Steel fibre ( $\text{€}/\text{Kg}$ ):  $\text{€ } 1.5 + \sigma = 30\%$ ;
- Steel bars ( $\text{€}/\text{Kg}$ ):  $\text{€ } 1.42 + \sigma = 10\%$ . [25]

A minimum point, more evident than ULS, in costs was found, which varies according to the requirements to be met at SLS. The Table 5.16 shows the precise information. It can be noted that for more restrictive limitations, from the economic point of view the traditional solution is widely replaced by a hybrid solution and in particular that which provides for a fiber dosage of  $50\text{Kg}/\text{m}^3$  and a percentage of ordinary reinforcement  $\rho_s$  equal to 0.2.

The cost of the fibres is higher than the cost of the reinforcement re-bars, nevertheless there is an indirect economic advantage: the reduction in construction time compared with the traditional one which provides the steel rebars installation on top and bottom. The variance is based on some considerations that were not taken into account in the average cost. Field data in fact support the thesis that FRC is advantageous because, for example, it can be directly pumped, in the case of elevated slabs, avoiding the costs of hiring adequate cranes for lifting the reinforcement; there is a clear physical simplification of the work that improves energy efficiency, better safety on site because some risks are eliminated, reduction in the staff involved in installation and finishing.

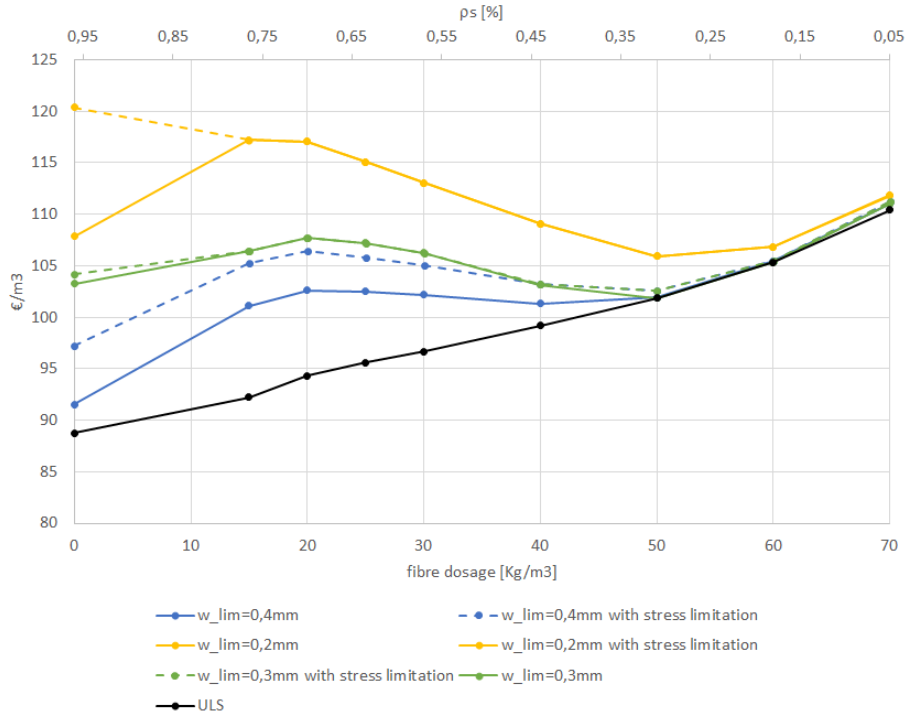


Figure 5.25: Oscillation average costs

LIMITATIONS		crack width		crack width and stress	
$w_{max}$	cost	solution	€/m <sup>3</sup>	solution	€/m <sup>3</sup>
0.4	max		76.63		76.65
	average	OCR	91.52	HRC6.9	101.83
	min		100.67		113.6
0.3	max		76.95		76.95
	average	OCR	97.18	HRC6.9	102.52
	min		106.90		114.62
0.2	max		78.17		78.17
	average	HRC6.9	105.93	HRC6.9	105.93
	min		118.66		131.52

Table 5.16: Oscillation costs



## Chapter 6

# Conclusion and future studies

### 6.1 Conclusions about use of fibre

Fibre reinforcement extends the versatility of concrete as a construction material by overcoming the otherwise intrinsic brittleness and by improving the structural behaviour (crack propagation, flexural stiffness, ductility, ect), but also by the potential it has to simplify the construction process. In particular, the results presented and discussed in this work thesis yield the following conclusions:

1. Reinforcement solutions considered, calculated with an easy and straightforward procedure for the designing of Hybrid Reinforcement flat slab at ULS based on performing a plastic analysis of the structure using a plastic moment design method, do not in most cases verify the limitations dictated by the regulations in terms of maximum control crack width and tension;
2. By fixing a percentage of reinforcement  $\rho_s$  and changing the quantity of fibre (or  $f_{R3k}$ ), a positive contribution of the fibre to the control crack width is evident;
3. Fibres help to reduce steel tensions by contributing to the verification of maximum tensions, but in FRC solutions they are not capable of meeting SLS requirements, since the greatest contribution is provided by the bars;

4. Class *b*, *c*, *d* fibres, respectively  $f_{R3k}/f_{R1k}$  equal to 0.75, 1, 1.3, respond in different way to crack control and in particular no beneficial effects can be found in classes *c* and *d*, where as the percentage of reinforcement  $\rho_s$  decreases and the fibre dosage  $f_{R3k}$  increases, it was however necessary to design a greater reinforcement to verify the SLS;
5. For type *b* fibres, by increasing the fibre dosage (or  $f_{R3k}$ ) and decreasing the percentage of reinforcement  $\rho_s$ , it is possible to identify ranges of values ( $f_{R3k}= 2.7 - 6.9$  Mpa and respectively  $\rho_s=0.6-0.26$ ) according to which the quantities of steel designed are gradually more advantageous to respond to SLS;
6. Considering the fiber class *b*, the HRC solutions designed meet the requirements of SLS with no or minimum additional reinforcement, for fiber dosages of  $50Kg/m^3$ ,  $f_{R3k}= 6.9$  Mpa and  $\rho_s=0.26$ ;
7. Where the maximum crack opening is 0.4mm from an economic point of view, the traditional solution (OCR) is more convenient, while for more restrictive values, optimisation points can be identified in HRC solutions.

## 6.2 Future studies

The verification of the maximum crack opening and tensions are the basis for any concrete project. Future studies may focus on the investigation of more complicated concrete phenomena or on the management of the product life cycle and its impact. More precisely, the issues could be:

- the study of the behavior of such solutions, expected for elevated slabs, considering the effects of second order: such as creep and shrinkage;
- the study of the behavior of HRC if you consider multiple fiber mixes in order to improve certain aspects such as the addition of additives in concrete to improve for instance the compatibility;
- the study of the sustainability of this design choice in terms of: environment, society and economy;
- the analysis of HRC solution from the point of view of the L.C.A. (Life Cycle Assessment) and L.C.M. (Life Cycle Management).

# Annexes

## Annex A: Newton Raphson algorithm

For the calculation of crack width it is required to obtain the strain plane of the section in question for applied  $N_{est}-M_{est}$  what, in turn, provides the information of produced stressed due to the established constitutive laws of the specified materials. The seek of mentioned strain plane could be carried out by means of Newton-Raphson method. It is an iterative calculation with the aim of balancing the internal forces generated by produced internal stresses with the external forces. Briefly, the Newton-Raphson method is a quick way to find a good approximation for the solution of a real-valued function  $f(x) = 0$ , using the idea that a continuous function can be approximated by a series of tangents of  $f(x)$  (Figure 6.1). The algorithm foresees a number of iterations: The algorithm foresees a number of iterations:

$$k = 1, 2, 3, \dots n$$

. Each approximation  $x_k$  is given by the intersection between the tangent line  $t_{(k-1)}$  to the function  $f(x)$ , at the point  $(x_{k-1}, f(x_{k-1}))$ , and  $y = 0$ .

$$t_{(k-1)} = y = f(x_{k-1}) + f'(x_{k-1})(x - x_{k-1})$$

Imposed  $x_0$  and  $y = 0$ :

$$x_k = x_{k-1} - \frac{f(x_{k-1})}{f'(x_{k-1})}, k = 1, 2, \dots n \quad (6.1)$$

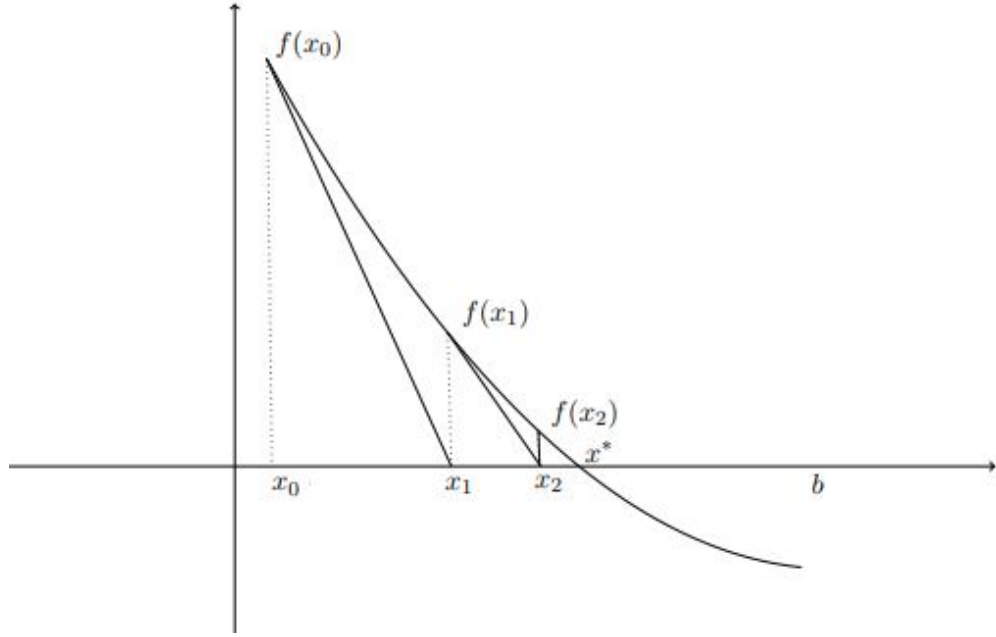


**Figure 6.1:** Newton Rapshon method

In the presented study there are two roots to be found which are:  $f_1(x, y) = (N_{int} - N_{est})$  and  $f_2(x, y) = (M_{int} - M_{est})$ . It should be pointed out that the system of equations is to be resolved what means that the found stain plane should provide the equilibrium as for applied axial force so for the applied moment satisfy simultaneously the N-M equilibrium with external forces. In order to find the required strain plane, at least two points must be found which were established as:  $x$ - strain at the top fibre of section ( $\varepsilon_t$ ) and  $y$ - the bottom one ( $\varepsilon_b$ ). A tolerance has been agreed in the solution of  $\epsilon = 10^{-5}$ . The bi-dimensional problem is presented in Equation 6.2.

$$\begin{pmatrix} f_1(x, y) \\ f_2(x, y) \end{pmatrix} = \begin{pmatrix} N_{int}(\varepsilon_t, \varepsilon_b) - N_{est} \\ M_{int}(\varepsilon_t, \varepsilon_b) - M_{est} \end{pmatrix} = \begin{pmatrix} 10^{-5} \\ 10^{-5} \end{pmatrix} = \begin{pmatrix} \epsilon_1 \\ \epsilon_2 \end{pmatrix} \quad (6.2)$$

The algorithm implemented in Matlab follows the Figure 6.2.

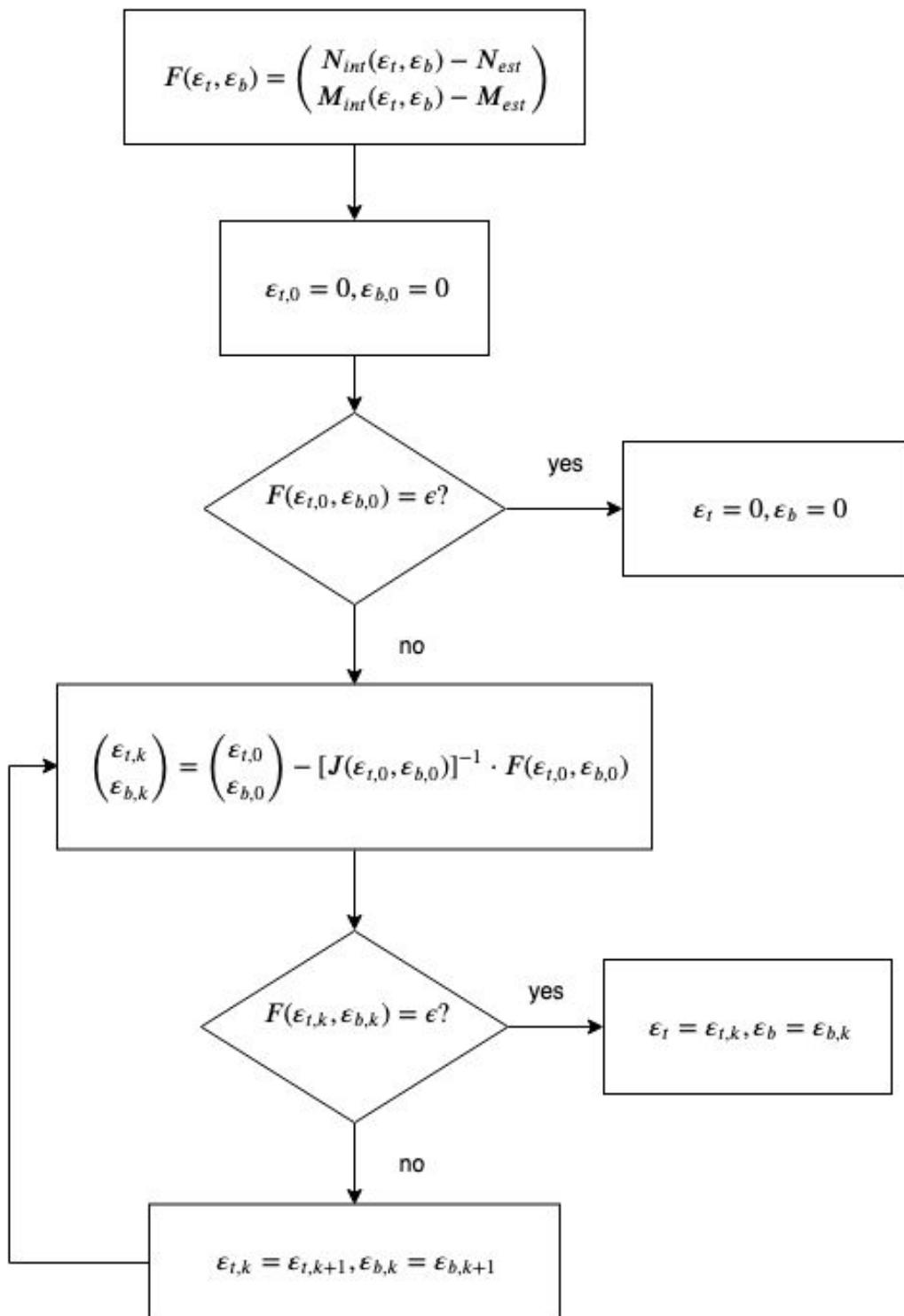


Figure 6.2: Newton Raphson algorithm



# Acronyms

- $G_f$  fracture energy of plain concrete. 20
- $M_{cr}$  cracking moment. 27, 33, 52
- $M_{est}$  External bending moment. 35, 52, 79
- $N_{est}$  Internal axil. 35, 52, 79, 80
- $W_I$  section modulus of the element. 27
- $\alpha_{cc}$  long-term load application coefficient. 36
- $\phi_f$  fibre diameter. 6
- $\phi_s$  diameter steel bar. 28
- $\rho_{s,ef}$  effective reinforcement ratio ( $= A_s/A_{c,ef}$ ). 28
- $\rho_s$  effective reinforcement ratio ( $= A_s/A_c$ ). 72, 77, 78
- $\sigma_{sr}$  the maximum steel stress in a crack formation stage. 8
- $\sigma$  stress. 8, 17, 18
- $\tau_{bm}$  mean bond strength between steel and concrete. 28
- $\varepsilon_{Fu}$  fibre ultimate strain. 19
- $\varepsilon_{cr}$  crack concrete strain. 26
- $\varepsilon_{cu}$  ultimate strain concrete. 8, 10
- $\varepsilon_{su}$  ultimate strain steel. 8
- $\varepsilon_{uk}$  ultimate characteristic strain. 13

$\varepsilon_{yk}$  characteristic yield strain steel. 13

$\varepsilon$  strain. 8, 13, 18

$c$  cover. 29

$f_{Fts}$  serviceability flexural residual strength. 16, 87

$f_{Ftu}$  ultimate flexural residual strength. 9, 16, 87

$f_{R,j}$  residual flexural tensile strength corresponding to  $CMOD_j$ . 15

$f_{R1k}$  flexural residual strength  $CMOD=0.5mm$ . 15, 16

$f_{R3k}$  flexural residual strength  $CMOD=2.5mm$ . 15, 16, 66, 77, 78

$f_{cd}$  design compressive strength concrete. 10, 36

$f_{ctm}$  mean tensile strength of concrete. 12

$f_{ct}$  tensile strength of concrete. 14, 28

$l_{cs}$  fibre characteristic length. 7, 8, 18

$l_f$  fibre length. 6, 7

$l_t$  transfer length. 28, 33

$s_{rm}$  mean distance value between cracks. 28

$w_d$  width crack opening design. 9, 37

$x_n$  neutral axis. 18

**ACI** American Concrete Institute. 3

**CMOD** Crack Mouth Opening Displacement. 15

**fib MC10** fib Model Code 2010. 10, 12, 32, 33, 36

**FRC** Fibre Reinforced Concrete. 1–4, 8, 14

**HRC** Hybrid Reinforced Concrete. xi, 26

**OR** ordinary steel reinforcement. 9, 18

**ORC** ordinary steel reinforcement concrete. 26

**SFRC** Steel Fibre Reinforced Concrete. xi, 4, 7, 9, 14, 18, 21, 26, 41

**SLS** Serviceability Limit State. 1, 2, 9, 10, 13, 21, 35, 37, 50, 63, 77, 78

**ULS** Ultimate Limit State. 2, 10, 13, 17, 21, 35, 36, 50, 57, 77



# List of Figures

2.1	General diagram load/crack width for fibre-reinforced and no reinforced matrix . . . . .	5
2.2	Types fibres steel . . . . .	7
2.3	Plane strain for ORC . . . . .	9
2.4	Schematic representation of the stress–strain relation for structural concrete [7] . . . . .	10
2.5	Parabola–rectangle diagram for concrete in compression . . . . .	11
2.6	Design stress strain relations for various concrete strength classes	12
2.7	Steel behaviour . . . . .	13
2.8	Softening (a) and Hardening (b) behaviour [7] . . . . .	14
2.9	3-point bending test, set up required by EN 14651 . . . . .	15
2.10	Typical load F-CMOD curve for plain concrete and FRC . . . . .	16
2.11	Stress diagrams for the determination of the residual tensile strength $f_{Fts}$ (a) and $f_{Ftu}$ (b) for linear model, respectively . . . . .	16
2.12	Rigid-plastic model . . . . .	17
2.13	Simplified post-cracking constitutive laws: hardening(dashed line) and softening (continuous line) . . . . .	18
2.14	Stress-strain relation for softening behaviour of FRC . . . . .	19

2.15	Stress-strain relationship for hardening behaviour [14] . . . . .	20
2.16	Drawing of the coordinates:(a) Linear elastic model hardening behaviour, (b) Linear elastic model softening behaviour (c) Rigid plastic model . . . . .	22
3.1	Tension-average steel strain in all phases [17] . . . . .	27
3.2	Transfer length [17] . . . . .	28
3.3	Crack spacing - Load . . . . .	29
3.4	Detail of a crack . . . . .	30
3.5	Transfer length in FRC [17] . . . . .	31
3.6	Strains around FRC crack . . . . .	31
3.7	Stress steel reduction due to presence fibers . . . . .	32
4.1	M-N envelopes for different constitutive laws at ULS . . . . .	36
4.2	M-N envelopes for different sectional depths [mm] at ULS (Sar- gin's parabola-linear elastic model) . . . . .	37
4.3	M-N envelopes for different $w_d$ [mm] at SLS (Sargin's parabola- linear elastic model) . . . . .	38
4.4	Limitation for elastic linear model at SLS for different wd . . . . .	38
4.5	FRC40-4c h=300mm wd=0.3. Comparation ULS-SLS . . . . .	39
4.6	FRC40-3c h=300mm wd=0.4. Comparison models . . . . .	40
4.7	M-N envelopes for plain concrete, FRC, ordinary reinforced concrete and mix solution at ULS . . . . .	41
4.8	M-N envelopes for FRC40-6b and 4c with and without ordi- nary reinforcement . . . . .	42
5.1	Model geometry . . . . .	44

5.2	Collapse mechanisms for flat slab [8] . . . . .	46
5.3	Top reinforcement distribution . . . . .	47
5.4	Total amount of steel (fibre+rebar) in relation to $f_{R3k}$ . . . . .	50
5.5	Elastic moment distribution in quasi-permanent load combination . . . . .	51
5.6	Load-Moment relationship for the structure in question . . . . .	52
5.7	Amount of fibre - Crack width for different $\rho_s$ . External panel. $M_{qp} = 88.8KNm$ . Ratio 0.75 . . . . .	54
5.8	Amount of fibre - Crack width for $\rho_s=0.4$ and different class fibre. External panel. $M_{qp} = 88.8KNm$ . . . . .	55
5.9	Applied Load - Crack Width relationship for established Hybrid Solution HRC4.1-0.4 (int) . . . . .	56
5.10	Comparison of crack width for positive and negative moment, internal and external panel, reinforcement HRC4.1 . . . . .	57
5.11	Applied Load - Crack Widths for different Hybrid Solutions . . . . .	59
5.12	Recommended values of $w_{max}$ (mm) [15] . . . . .	60
5.13	Applied Load - Crack Widths verification for different Hybrid Solutions. External panel . . . . .	62
5.14	Applied Load - Crack Widths verification for different Hybrid Solutions. Internal panel . . . . .	63
5.15	Designed amount of traditional reinforcement at SLS ( $f_{R3k}/f_{R1k}=0.75$ ). External panel . . . . .	65
5.16	Ratio ( $A_{s,SLS}/A_{s,ULS}$ ) of quantity of steel bars reinforcement added. Ratio 0.75. . . . .	67
5.17	Total steel content. Maximum crack width 0.2 mm . . . . .	68
5.18	Total steel content. Maximum crack width 0.3 mm . . . . .	69
5.19	Total steel content. Maximum crack width 0.4 mm . . . . .	69

5.20	Optimization points: $f_{R3k-\rho_s}$ . . . . .	71
5.21	Optimization points: $f_{R3k-kg/m^3}$ . . . . .	71
5.22	Total steel content. Maximum crack width= 0.2mm and stress limitation . . . . .	72
5.23	Total steel content. Maximum crack width= 0.3mm and stress limitation . . . . .	73
5.24	Total steel content. Maximum crack width= 0.4mm and stress limitation . . . . .	73
5.25	Oscillation average costs . . . . .	75
6.1	Newton Raphson method . . . . .	80
6.2	Newton Raphson algorithm . . . . .	81

# List of Tables

2.1	Fibre sub-classes . . . . .	5
2.2	A compilation of mechanical properties of commonly used fibres in concrete materials[8] . . . . .	6
2.3	Main points for trilinear tensioned concrete softening behaviour	20
2.4	Main points for trilinear tensioned concrete hardening behaviour	21
2.5	Safety factors . . . . .	21
2.6	Examples . . . . .	22
2.7	Values coordinates $\sigma - \epsilon$ . . . . .	23
5.1	Model properties . . . . .	44
5.2	Top reinforcement distribution (E.D.= edge distance is the centerline of the column to the edge of slab) . . . . .	47
5.3	Fibre properties [23] . . . . .	48
5.4	Amount of top and bottom reinforcement in the optimised hybrid flat slab for $mm^2/m$ at ULS . . . . .	49
5.5	Total steel content in the optimised hybrid flat slab at ULS $Kg/m^3$ . . . . .	49
5.6	Quasi-permanent combination load[24] . . . . .	51

5.7	Applied load/produced external moment . . . . .	53
5.8	Applied Load - Crack Widths for different reinforcement solutions . . . . .	58
5.9	Recommendation for SFRC $w_{max}$ [mm] . . . . .	60
5.10	Crack width in internal and external panel at $M_{qp}^-$ for different ratio. Maximum crack width= 0.4mm . . . . .	61
5.11	Crack width in internal and external panel at $M_{qp}^-$ for different ratio. Maximum crack width= 0.3mm . . . . .	61
5.12	The required amount of additional reinforcement at SLS ( $w_{max}=0.2\text{mm}$ , $f_{R3k}/f_{R1k}=0.75$ ) . . . . .	64
5.13	The required amount of additional reinforcement at SLS ( $w_{max}=0.3\text{mm}$ , $f_{R3k}/f_{R1k}=0.75$ ) . . . . .	64
5.14	The required amount of additional reinforcement at SLS ( $w_{max}=0.4\text{mm}$ , $f_{R3k}/f_{R1k}=0.75$ ) . . . . .	65
5.15	Total steel content: fibre + rebars $kg/m^3$ . . . . .	68
5.16	Oscillation costs . . . . .	75

# Bibliography

- [1] J. Romualdi and G. Batson, *Mechanics of Crack Arrest in Concrete*. ASCE. 89, J. Engineering Mechanics, 1963.
- [2] J. Romualdi and J. Mandel, *Tensile Strength of Concrete Affected by Uniformly Distributed and Closely Spaced Short Lengths of Wire Reinforcement*. Vol. 61, Journal of the American Concrete Institute, 1964.
- [3] H. Krenchel, *Fibre Reinforcement*. English translation, Copenhagen, Denmark: Akademisk Forlag, 1964.
- [4] M. Stahlfaserbeton, *DBV*. Germany: Deutsche Beton Vereneis, 2001.
- [5] R. T. 162-TDF.,  $\sigma - \varepsilon$  design method. *Final Recommendation*. Materials and structures, Vol. 36, 2003.
- [6] C.N.R., *Istruzioni per la Progettazione, l'Esecuzione ed il Controllo di Strutture di Calcestruzzo Fibrorinforzato*. DT 204, 2008.
- [7] *Eurocode 02 - Reinforced Concrete Design*. 2004.
- [8] A.C.I., *Report on the Physical Properties and Durability of Fiber-Reinforced Concrete*. Rep. 544.5R-10, Farmington Hills, MI: Reported by ACI Committee, 544, 2010.
- [9] M. del fomento, *EHE-08, Instrucion de Hormigon Estructural*, 2008.
- [10] B. Espion and X. Destrée, *Test report of loading up to failure of five fiber reinforced concrete (FRC) slabs*. 2004.
- [11] A. D. la Fuente, R. Escariz, *et al.*, *Design of macro-synthetic fibre reinforced concrete pipes*. Construction and Building Materials, June 2013.

- [12] J. A. Barros *et al.*, *Post-cracking behaviour of steel fibre reinforced concrete. Materials and Structures*. 38(1), Reported by ACI Committee, 544, 2005.
- [13] A. Jansson, *Fibres in reinforced concrete structures-analysis, experiments and design*. Thesis, Göteborg, Sweden 2008: Department of Civil and Environmental Engineering, 2008.
- [14] CEB and FIP, *fib Model Code for Concrete Structures*. final draft, 2010.
- [15] *EN 14651, Concrete Tension Testing*. 2007.
- [16] A. Fantilli *et al.*, *Behaviour of R/C elements in bending and tension: the problem of minimum reinforcement ratio*. Materials and Structures, 2006.
- [17] G. Groli, *Crack width control in RC elements with recycled steel fibres and applications to integral structures: theoretical and experimental study*. Polytechnic University of Madrid, 2014.
- [18] A. Perèz, *Estudio de fisuraciòn en muros pantalla-Informe final*. CDTI, 2010.
- [19] A. B. J.B. Read *et al.*, *An investigation of the crack control characteristics of various types of bars in reinforced concrete*. Cement and Concrete Association, 1966.
- [20] R. Cederhout, *Crack width control reinforced steel fibre concrete-Influence of steel fibres of the crack width*. TU Delft and Gemeente Rotterdam, 2012.
- [21] L. Sutera, *Optimization of Hybrid Flat Slab*. Master thesis, Barcelona: Department of Civil and Environmental Engineering-Polytechnic of Turin/Catalunya, 2019.
- [22] C. G. Kennedy, *Practical yield line design*. Fiz. i Khimiya Obrab. Mater, 2003.
- [23] G. Plizzari, F. Minelli, *et al.*, “Elevated slabs made of hybrid reinforced concrete: Proposal of a new design approach in flexure,” vol. 20, 2019.
- [24] *Norme Tecniche Costruttive*. 2018.
- [25] I. de Tecnología de la Construcción, “Bedec,” 2019.

# Acknowledgements

Al termine di questo percorso sento di dover ringraziare molte persone che ho incontrato durante questa magistrale che è iniziata come un'avventura ed è finita come una sfida che sento di aver superato, non tanto per ciò che ho ottenuto, quanto per le esperienze che ho vissuto, ciò che ho affrontato e appreso.

Un doveroso ringraziamento va a al professor Albert De la Fuente e a Stanislav Aidarov per avermi guidato durante questo lavoro di tesi, per la loro immensa disponibilità e per avermi ripetuto "ánimo!" durante questi mesi. Al professor Pasquale Fantilli per aver appoggiato le nostre idee.

Grazie a tutta la mia famiglia, che mi ha sostenuta e apprezzata nelle vittorie e ha continuato a farlo anche nelle sconfitte. Grazie a Vincenzo e Saba, per essere stati il punto di partenza e riferimento nella mia esperienza spagnola. Ma soprattutto, grazie a mia Madre e a mio Padre, che mi hanno permesso di realizzare ciò che volevo e si sono fidati dei miei progetti e delle mie decisioni. A mio fratello Antonello, che con i suoi modi di fare agli antipodi dai miei, contribuisce a migliorare, ogni giorno di piú, la mia autoironia. Questo traguardo è per voi!

Grazie agli amici che ci sono sempre stati, nonostante siamo ormai un po' distanti: Roberta, Micaela, Donato, Alecris, Vito e Nic per non essersi mostrati mai sordi ad ogni mia chiamata. Grazie anche a Davide che mi ha riservato parole giuste, come se conoscesse il peggio di me, da una vita; e a Manuel per aver sempre aggiunto quella dose di razionalità, che spesso mi manca.

Agli amici di Torino, che è stato tanto difficile lasciare quando le nostre strade si sono dovute separare. Torino può essere più bella di Barcellona, quando hai dei bellissimi ricordi e delle persone con cui hai condiviso dei

bellissimi momenti. Grazie Alexia, Chiri, Leo, Supersimo, Kawtar, Peppe, la mia prima casa "CRU136" e i "rematori professionisti". Grazie a Stefania per essere, in qualsiasi città, una stella polare (dopo un paio di semafori!). Grazie ad Adriana, con cui ho condiviso tanti gelati, ma anche tanti momenti in cui ci siamo trovate davanti ai nostri limiti e abbiamo dovuto ricordarci a vicenda che sappiamo prenderci tutto quello che vogliamo, anche quando i denti sono già abbastanza stretti. A quello che è stato via Santa Chiara.

Agli amici conosciuti a Barcellona: Teresa, Alberto, Francesco, Luca M., Aldo, Simone e Veronica; che mi hanno accettata con ogni mia stramberia, compresa quella di non essere mai stata al Razzmataz o non avere mai piani.

Infine, il grazie più grande lo devo a Luca e Andrea, senza il loro prezioso aiuto e supporto morale, questo lavoro di tesi non si sarebbe mai concluso. Grazie per avermi letteralmente adottata e sopportato. In particolare: grazie Andrea per avermi aiutato a farmi sentire a casa in un momento particolarmente buio e anche per avermi fatto disperare davanti alle tue idee troppo informatiche. Grazie Luca per i mesi passati insieme, per i nostri scambi di opinioni sinceri ma poco pacifici, per la tua pazienza e per aver sacrificato la tua tranquillità, i tuoi silenzi e il tuo tempo, in cambio dei miei innumerevoli lamenti. Eres mi piulo favorito!

Dedicare poche righe ad ognuno non sarà mai sufficiente per esprimere il mio affetto e la mia gratitudine, tuttavia conserverò gelosamente i ricordi di tutti i momenti belli passati insieme a tutte le persone che ancora ci sono e anche quelle che non fanno più parte della mia quotidianità, ma che in qualche modo mi hanno lasciato qualcosa.

*Vi voglio bene.*

*Os quiero un montón.*

Manuela